



University Transportation Research Center - Region 2

Final Report



Activity-Based Approach for the Design of Sustainable Area and Cordon Pricing Schemes

Performing Organization: University of Puerto Rico, Mayagüez
The City University of New York (CUNY)



September 2018



Sponsor:
University Transportation Research Center - Region 2

University Transportation Research Center - Region 2

The Region 2 University Transportation Research Center (UTRC) is one of ten original University Transportation Centers established in 1987 by the U.S. Congress. These Centers were established with the recognition that transportation plays a key role in the nation's economy and the quality of life of its citizens. University faculty members provide a critical link in resolving our national and regional transportation problems while training the professionals who address our transportation systems and their customers on a daily basis.

The UTRC was established in order to support research, education and the transfer of technology in the field of transportation. The theme of the Center is "Planning and Managing Regional Transportation Systems in a Changing World." Presently, under the direction of Dr. Camille Kamga, the UTRC represents USDOT Region II, including New York, New Jersey, Puerto Rico and the U.S. Virgin Islands. Functioning as a consortium of twelve major Universities throughout the region, UTRC is located at the CUNY Institute for Transportation Systems at The City College of New York, the lead institution of the consortium. The Center, through its consortium, an Agency-Industry Council and its Director and Staff, supports research, education, and technology transfer under its theme. UTRC's three main goals are:

Research

The research program objectives are (1) to develop a theme based transportation research program that is responsive to the needs of regional transportation organizations and stakeholders, and (2) to conduct that program in cooperation with the partners. The program includes both studies that are identified with research partners of projects targeted to the theme, and targeted, short-term projects. The program develops competitive proposals, which are evaluated to insure the most responsive UTRC team conducts the work. The research program is responsive to the UTRC theme: "Planning and Managing Regional Transportation Systems in a Changing World." The complex transportation system of transit and infrastructure, and the rapidly changing environment impacts the nation's largest city and metropolitan area. The New York/New Jersey Metropolitan has over 19 million people, 600,000 businesses and 9 million workers. The Region's intermodal and multimodal systems must serve all customers and stakeholders within the region and globally. Under the current grant, the new research projects and the ongoing research projects concentrate the program efforts on the categories of Transportation Systems Performance and Information Infrastructure to provide needed services to the New Jersey Department of Transportation, New York City Department of Transportation, New York Metropolitan Transportation Council, New York State Department of Transportation, and the New York State Energy and Research Development Authority and others, all while enhancing the center's theme.

Education and Workforce Development

The modern professional must combine the technical skills of engineering and planning with knowledge of economics, environmental science, management, finance, and law as well as negotiation skills, psychology and sociology. And, she/he must be computer literate, wired to the web, and knowledgeable about advances in information technology. UTRC's education and training efforts provide a multidisciplinary program of course work and experiential learning to train students and provide advanced training or retraining of practitioners to plan and manage regional transportation systems. UTRC must meet the need to educate the undergraduate and graduate student with a foundation of transportation fundamentals that allows for solving complex problems in a world much more dynamic than even a decade ago. Simultaneously, the demand for continuing education is growing – either because of professional license requirements or because the workplace demands it – and provides the opportunity to combine State of Practice education with tailored ways of delivering content.

Technology Transfer

UTRC's Technology Transfer Program goes beyond what might be considered "traditional" technology transfer activities. Its main objectives are (1) to increase the awareness and level of information concerning transportation issues facing Region 2; (2) to improve the knowledge base and approach to problem solving of the region's transportation workforce, from those operating the systems to those at the most senior level of managing the system; and by doing so, to improve the overall professional capability of the transportation workforce; (3) to stimulate discussion and debate concerning the integration of new technologies into our culture, our work and our transportation systems; (4) to provide the more traditional but extremely important job of disseminating research and project reports, studies, analysis and use of tools to the education, research and practicing community both nationally and internationally; and (5) to provide unbiased information and testimony to decision-makers concerning regional transportation issues consistent with the UTRC theme.

Project No(s):

UTRC/RF Grant No: 49198-37-28, 49198-38-28

Project Date: September 2018

Project Title: Activity-Based Approach for the Design of Sustainable Area and Cordon Pricing Schemes

Project's Website:

<http://www.utrc2.org/research/projects/activity-based-approach-design-sustainable-area-and-cordon-pricing>

Principal Investigator(s):

Daniel Rodriguez-Roman, Ph.D.

Assistant Professor

University of Puerto Rico, Mayagüez

Mayagüez, PR 00681-9000

Email: daniel.rodriguez6@upr.edu

Mahdieh Allahvirraloo, Ph.D.

Assistant Professor

The City College of New York

160 Convent Avenue

New York, NY 10031

Email: mallahviranloo@ccny.cuny.edu

Performing Organization(s):

University of Puerto Rico, Mayagüez

The City University of New York (CUNY)

Sponsor(s):

University Transportation Research Center (UTRC)

To request a hard copy of our final reports, please send us an email at utrc@utrc2.org

Mailing Address:

University Transportation Research Center

The City College of New York

Marshak Hall, Suite 910

160 Convent Avenue

New York, NY 10031

Tel: 212-650-8051

Fax: 212-650-8374

Web: www.utrc2.org

Board of Directors

The UTRC Board of Directors consists of one or two members from each Consortium school (each school receives two votes regardless of the number of representatives on the board). The Center Director is an ex-officio member of the Board and The Center management team serves as staff to the Board.

City University of New York

Dr. Robert E. Paaswell - Director Emeritus of NY
Dr. Hongmian Gong - Geography/Hunter College

Clarkson University

Dr. Kerop D. Janoyan - Civil Engineering

Columbia University

Dr. Raimondo Betti - Civil Engineering
Dr. Elliott Sclar - Urban and Regional Planning

Cornell University

Dr. Huaizhu (Oliver) Gao - Civil Engineering
Dr. Richard Geddes - Cornell Program in Infrastructure Policy

Hofstra University

Dr. Jean-Paul Rodrigue - Global Studies and Geography

Manhattan College

Dr. Anirban De - Civil & Environmental Engineering
Dr. Matthew Volovski - Civil & Environmental Engineering

New Jersey Institute of Technology

Dr. Steven I-Jy Chien - Civil Engineering
Dr. Joyoung Lee - Civil & Environmental Engineering

New York Institute of Technology

Dr. Nada Marie Anid - Engineering & Computing Sciences
Dr. Marta Panero - Engineering & Computing Sciences

New York University

Dr. Mitchell L. Moss - Urban Policy and Planning
Dr. Rae Zimmerman - Planning and Public Administration

(NYU Tandon School of Engineering)

Dr. John C. Falocchio - Civil Engineering
Dr. Kaan Ozbay - Civil Engineering
Dr. Elena Prassas - Civil Engineering

Rensselaer Polytechnic Institute

Dr. José Holguín-Veras - Civil Engineering
Dr. William "Al" Wallace - Systems Engineering

Rochester Institute of Technology

Dr. James Winebrake - Science, Technology and Society/Public Policy
Dr. J. Scott Hawker - Software Engineering

Rowan University

Dr. Yusuf Mehta - Civil Engineering
Dr. Beena Sukumaran - Civil Engineering

State University of New York

Michael M. Fancher - Nanoscience
Dr. Catherine T. Lawson - City & Regional Planning
Dr. Adel W. Sadek - Transportation Systems Engineering
Dr. Shmuel Yahalom - Economics

Stevens Institute of Technology

Dr. Sophia Hassiotis - Civil Engineering
Dr. Thomas H. Wakeman III - Civil Engineering

Syracuse University

Dr. Baris Salman - Civil Engineering
Dr. O. Sam Salem - Construction Engineering and Management

The College of New Jersey

Dr. Thomas M. Brennan Jr - Civil Engineering

University of Puerto Rico - Mayagüez

Dr. Ismael Pagán-Trinidad - Civil Engineering
Dr. Didier M. Valdés-Díaz - Civil Engineering

UTRC Consortium Universities

The following universities/colleges are members of the UTRC consortium under MAP-21 ACT.

City University of New York (CUNY)
Clarkson University (Clarkson)
Columbia University (Columbia)
Cornell University (Cornell)
Hofstra University (Hofstra)
Manhattan College (MC)
New Jersey Institute of Technology (NJIT)
New York Institute of Technology (NYIT)
New York University (NYU)
Rensselaer Polytechnic Institute (RPI)
Rochester Institute of Technology (RIT)
Rowan University (Rowan)
State University of New York (SUNY)
Stevens Institute of Technology (Stevens)
Syracuse University (SU)
The College of New Jersey (TCNJ)
University of Puerto Rico - Mayagüez (UPRM)

UTRC Key Staff

Dr. Camille Kamga: *Director, Associate Professor of Civil Engineering*

Dr. Robert E. Paaswell: *Director Emeritus of UTRC and Distinguished Professor of Civil Engineering, The City College of New York*

Dr. Ellen Thorson: *Senior Research Fellow*

Penny Eickemeyer: *Associate Director for Research, UTRC*

Dr. Alison Conway: *Associate Director for Education/Associate Professor of Civil Engineering*

Nadia Aslam: *Assistant Director for Technology Transfer*

Nathalie Martinez: *Research Associate/Budget Analyst*

Andriy Blagay: *Graphic Intern*

Tierra Fisher: *Office Manager*

Dr. Sandeep Mudigonda, *Research Associate*

Dr. Rodrigue Tchamna, *Research Associate*

Dr. Dan Wan, *Research Assistant*

Bahman Moghimi: *Research Assistant;*
Ph.D. Student, Transportation Program

Sabiheh Fagigh: *Research Assistant;*
Ph.D. Student, Transportation Program

Patricio Vicuna: *Research Assistant*
Ph.D. Candidate, Transportation Program

Disclaimer

The contents of this report reflect the views of the authors, who are responsible for the facts and the accuracy of the information presented herein. The contents do not necessarily reflect the official views or policies of the UTRC. This report does not constitute a standard, specification or regulation. This document is disseminated under the sponsorship of the US Department of Transportation, University Transportation Centers Program, in the interest of information exchange. The U.S. Government assumes no liability for the contents or use thereof.

1. Report No.	2. Government Accession No.	3. Recipient's Catalog No.	
4. Title and Subtitle Activity-Based Approach for the Design of Sustainable Area and Cordon Pricing Schemes		5. Report Date: September 2018	
7. Author(s) <i>Daniel Rodriguez-Roman, PhD</i> Assistant Professor University of Puerto Rico, Mayagüez <i>Mahdieh Allahvirraloo, PhD</i> Assistant Professor City College of New York		6. Performing Organization Code	
9. Performing Organization Name and Address University of Puerto Rico, Mayagüez PO BOX 9000 Mayagüez, PR 00681-9000 The City College of New York 160 Convent Avenue New York, NY 10031		8. Performing Organization Report No.	
12. Sponsoring Agency Name and Address University Transportation Research Center 160 Convent Avenue, Marshak Hall 910 New York, NY 10031		10. Work Unit No.	11. Contract or Grant No. 49198-37-28, 49198-38-28
15. Supplementary Notes		13. Type of Report and Period Covered	
16. Abstract Vehicle-generated emissions remain a serious threat to the health of urban and suburban communities. Among the strategies implemented to address this environmental problem are area- and cordon-based pricing (ACP) schemes. Experiences in major cities such as London, Stockholm, and Milan show that ACP schemes are effective in reducing traffic emissions and the related public health risks. However, designing ACP schemes continues to be a challenging task given the complexities of estimating the effects of this type of strategy. In response to this design problem, optimization-based approaches have been proposed to aid transportation planning agencies in determining optimal charging boundary locations and toll levels. Existing engineering methodologies focus only on congestion-related goals, as well as employing an aggregate representation of travel demand corresponding to a single design period (e.g., the morning peak hour). The existing models, however, do not account for the impacts of ACP schemes on pollutant distribution throughout the day, nor the resulting effects the levels of pollutant exposure experience by the public. In this project an ACP design approach is proposed that considers: a) the effects on pollutant concentrations of the pricing scheme, b) the effects on travelers' activity, schedule, and time-use preferences at a disaggregate level, c) the space-time distribution of pollutants along with the space-time distribution of travelers, and d) planning goals related to system-wide congestion levels and public health. Two types of planning problems are considered. In the first problem, it is assumed that the decision-maker is interested in designing a pricing schemes that achieves a mobility-related goal, while simultaneously reducing pollutant concentration levels below a pre-established threshold. The second problem adds an environmentally-oriented objective to the decision-makers plans. For the purpose of simulating the human exposure of pollutants at the level of individual agents, a new activity-based travel model is presented. The proposed ACP design problems are formulated as bi-level, simulation-based optimization problems. A problem's upper-level is composed of the policy makers' goals, which guide the selection of charging boundary's location and its associated tolling levels. The travelers' response to the policy maker's decisions, as well as the resulting system-wide impacts, are analyzed in the lower-level. The lower-level model system is composed of five sub-models: (a) models to simulate the travel behavior changes caused by the pricing scheme, (b) a traffic assignment model to estimate the distribution of traffic in the network, (c) a traffic emissions model, (d) a pollutant dispersion model, and (e) a pollutant exposure model. To solve the proposed design problems, two surrogate-based solution heuristics are proposed. A series of numerical tests are presented to illustrate the application and performance of the proposed methodology.		14. Sponsoring Agency Code	
17. Key Words		18. Distribution Statement	
19. Security Classif. (of this report) Unclassified	20. Security Classif. (of this page) Unclassified	21. No of Pages 42	22. Price

Table of Contents

List of Tables	ii
List of Figures.....	ii
Abstract.....	1
1 Introduction	2
2 Overview of Previous Studies	4
2.1 Environmentally-oriented road pricing	4
2.2 NDPs for the Design of ACP Schemes	4
2.3 Applications of Surrogate-Based Optimization in Transportation Planning and Engineering	5
2.4 Overview of ABMs.....	6
3 Methodology.....	7
3.1 General Problem Formulations	7
3.1.1 Singe-Objective Area Pricing Problem.....	7
3.1.2 Bi-Objective Area Pricing Problem	8
3.1.3 Specification of Travel-Related Planning Objectives	8
3.1.4 Specification of Environmentally-Oriented Planning Objectives	9
3.2 Lower-Level Model System.....	10
3.2.1 Features of Model Lower Level Model System.....	10
3.2.2 The Household Activity Pattern Problem	12
3.2.3 Modeling Human Exposure to Pollutants	14
3.3 Heuristics for Solving Area Pricing Problems	14
3.3.1 Fitting and Using Surrogate Models	15
3.3.2 Representing the Charging Area	15
3.3.3 SBSH for Single-Objective Area Pricing Design Problems	16
3.3.4 SBSH for Multi-Objective Area Pricing Design Problems.....	21
4 Tests and Results	25
4.1 Test Problems Setup.....	25
4.1.1 Models	26
4.1.2 Algorithm Parameters	26
4.2 Results for the Surrogate Models' Accuracy and Correlation Tests	27
4.3 Results for Single-Objective Design Problem.....	29
4.4 Results for Bi-Objective Design Problem	33
5 Summary and Potential Research Opportunities	35
References	36

List of Tables

Table 1. Parameter Values used in the SBSH-MP Trial Runs	27
Table 2. Parameter Values used in the SBSH-MP Trial Runs	27
Table 3. Results for Cross-Validation Tests	28

List of Figures

Figure 1. Lower-level model system	11
Figure 2. Simplified lower-level model system.....	11
Figure 3. Example of activity pattern. Presents activity plan of 2 persons in the dimension of time and space. Person 1 relocates his shopping activity to another place once zone 2 is defined a cordon area.....	12
Figure 4. Simple polygon representation of charging boundary	16
Figure 5. Abridged Chicago Sketch Network.....	25
Figure 6. Confusion matrix for solution feasibility tests	29
Figure 7. Progression in average percent improvement relative to best initial designs for single-objective problems.....	31
Figure 8. Progression of the average diversity levels of the solution pool for the SBSH-SPs.....	32
Figure 9. Example of generated polygons in trial runs with the a) M^{CS} , b) M^{SQ} , and c) M^{Rev} objectives.....	33
Figure 10. Average improvement in dominated objective space	34
Figure 11. Example of the distribution of a pool of solutions' objective values for a trial run	34

Abstract

Vehicle-generated emissions remain a serious threat to the health of urban and suburban communities. Among the strategies implemented to address this environmental problem are area- and cordon-based pricing (ACP) schemes. Experiences in major cities such as London, Stockholm, and Milan show that ACP schemes are effective in reducing traffic emissions and the related public health risks. However, designing ACP schemes continues to be a challenging task given the complexities of estimating the effects of this type of strategy. In response to this design problem, optimization-based approaches have been proposed to aid transportation planning agencies in determining optimal charging boundary locations and toll levels. Existing engineering methodologies focus only on congestion-related goals, as well as employing an aggregate representation of travel demand corresponding to a single design period (e.g., the morning peak hour). The existing models, however, do not account for the impacts of ACP schemes on pollutant distribution throughout the day, nor the resulting effects the levels of pollutant exposure experience by the public.

In this project an ACP design approach is proposed that considers: a) the effects on pollutant concentrations of the pricing scheme, b) the effects on travelers' activity, schedule, and time-use preferences at a disaggregate level, c) the space-time distribution of pollutants along with the space-time distribution of travelers, and d) planning goals related to system-wide congestion levels and public health. Two types of planning problems are considered. In the first problem, it is assumed that the decision-maker is interested in designing a pricing schemes that achieves a mobility-related goal, while simultaneously reducing pollutant concentration levels below a pre-established threshold. The second problem adds an environmentally-oriented objective to the decision-makers plans. For the purpose of simulating the human exposure of pollutants at the level of individual agents, a new activity-based travel model is presented.

The proposed ACP design problems are formulated as bi-level, simulation-based optimization problems. A problem's upper-level is composed of the policy makers' goals, which guide the selection of charging boundary's location and its associated tolling levels. The travelers' response to the policy maker's decisions, as well as the resulting system-wide impacts, are analyzed in the lower-level. The lower-level model system is composed of five sub-models: (a) models to simulate the travel behavior changes caused by the pricing scheme, (b) a traffic assignment model to estimate the distribution of traffic in the network, (c) a traffic emissions model, (d) a pollutant dispersion model, and (e) a pollutant exposure model. To solve the proposed design problems, two surrogate-based solution heuristics are proposed. A series of numerical tests are presented to illustrate the application and performance of the proposed methodology.

1 Introduction

Despite the technological advances made in recent decades, motor vehicles continue to be a major source of air pollutants that significantly affect public health. Just in the US, vehicle emissions are estimated to account for 60,000 premature deaths each year, making road transportation the deadliest sector in terms of air pollution-related mortality (Caiazzo et al., 2013). Worldwide, it is estimated that 150,000 people die each year from diseases caused by exposure to vehicle-generated air pollutants, a figure that could dramatically increase with continued trends in urbanization and car ownership in the developing world (World Bank, 2010). Motor vehicles also are a major source of emissions that contribute to climate change. Globally, motor vehicles are estimated to produce 10% of greenhouse gas (GHG) emissions, but in the US the road transportation sector is responsible for 23% of GHG emissions (OECD/ITF, 2010; US EPA, 2014).

How can cities reduce vehicle-generated air pollutants? Since at least the early 20th century, economic theory has pointed to road pricing as a response to the negative externalities of road transportation. Several cities have shown that, in practice, pricing is indeed an effective strategy. For example, a major implementation of a road pricing scheme is London's congestion charging zone, which decreased particulate matter emissions by approximately 10 percent (Tonne et al., 2008). In Stockholm a congestion charging system resulted in air pollutant reductions of around 10 percent (Eliasson et al., 2009). And, Milan's area pricing scheme produced comparatively positive results, including a 23 percent reduction in the concentration of particulate matter within the charging area (Rotaris et al., 2010). The previous cases are examples of area- and cordon-based pricing (ACP) schemes. Ongoing concerns regarding pollution levels in urban regions continue to drive interest in ACP schemes, as evidenced by the ACP proposals under consideration in New York City and Los Angeles (Fix NY, 2018; SCAG, 2016).

There are, however, major technical challenges in planning an effective road pricing scheme. To aid decision-makers in the design of ACP schemes, transportation engineers have proposed a series of network design problems (NDPs) focused on congestion reduction. These problems are characterized, in part, by aggregate representations of travel demand for a single time period (e.g., peak hours). Existing ACP model formulations do not account for (a) travelers' mobility behavior and activity patterns in relation to a pricing scheme, (b) the effects of ACP schemes on emissions and pollutant concentrations, and (c) the resulting variations in human pollutant exposure. In addition, available ACP models and solution algorithms are only applicable to single-objective problems, while decision makers interested in achieving both mobility and environmental sustainability goals must weigh multiple, potentially conflicting, objectives.

Given the potential environmental benefits of road pricing and the limitations of existing NDPs, a novel optimization-based approach to the design of sustainable ACP schemes is proposed in this report. The models in this report:

- Can be used to design ACP schemes that have a single or multiple planning objectives.
- Account for mobility goals of both policy makers and travelers, as well as the public health concerns associated with traffic emissions.
- Consider the design of ACP schemes under environmental constraints
- Integrate activity-based models to simulate scheduling and mode choice behavior
- Determine charging boundaries and toll levels that shift individuals' travel choices in space and time so that human exposure to traffic pollutants and total travel disutility are minimized.

In addition, two heuristics are presented in this report to solve single and multi-objective NDP for the design of ACP schemes. The heuristics employ a technique (surrogate-based optimization, SBO) that attempts to accelerate the discovery of good design solutions, a problem of practical concerns given the considerable computing requirements that ACP design problems can require.

Besides this introduction, this report is composed of five sections.

- *Section 2: Overview of Previous Studies.* A review of relevant literature is presented in Section 2. This review includes a discussion of environmentally-oriented NDP models for road pricing

schemes, a summary of existing methods for the design ACP schemes, and an overview of activity-based models (ABM) used to study and describe people's travel behavior.

- *Section 3: Methodology.* In this section the planning models for the design of ACP schemes are introduced. These models include single- and multi-objective formulations of the ACP planning problem. Furthermore, the different components of the model systems needed to design ACP schemes are discussed. The model system comprises five sub-models to simulate: traffic flows; traffic emissions; pollutant concentrations; activity participation, activity scheduling, and mode choice; and human exposure to pollutants. The section ends with a step-by-step description of the proposed solution heuristics.
- *Section 4: Tests and Results.* An illustrative application of the proposed models and solution heuristics is included in Section 4. Results are shown for tests of: (a) the predictive accuracy of four surrogate model types, (b) the performance of the heuristics proposed for the single-objective problems, and (c) the performance of the heuristic proposed for multi-objective ACP problems.
- *Section 5: Conclusion.* A summary of the methodological advances proposed in the report is presented in Section 5. In addition, future research directions are identified.

2 Overview of Previous Studies

Considerable work has been conducted on: (a) the development of environmentally-oriented NDPs for the design of road pricing schemes, (b) optimization-based methods for designing ACP schemes, (c) SBO approaches to solve transportation engineering problems, and (d) the modeling of human activity participation and scheduling behavior. An overview of this literature is presented next.

2.1 Environmentally-oriented road pricing

A defining feature of ACP schemes is the existence of a closed charging boundary that encircles the charging area; all vehicles crossing (cordon-based scheme) or driving within (area-based scheme) the charging boundary must pay a toll. In contrast, other pricing schemes consists of a series of tolled roads or intersections with no closed boundary requirements. For these types of schemes researchers have proposed the toll level setting problem (TLSP) and the toll design problem (TDP). It is assumed that in the TLSP a planning agency has already decided in which roads the tolls will be levied, and the design problem consists of determining the tolling level on the selected roads. In the TDP, both the tolling location and the tolling level must be determined. Environmentally-oriented versions of the TLSP and the TDP have been studied.

One of the most common and practical considerations in environmentally-oriented road pricing problems are environmental constraints, usually defined on the basis of environmental air quality regulations that establish maximum air pollutant concentrations thresholds. In NDPs with environmental constraints, the goal is to find a tolling scheme that optimizes a given planning objective (e.g., minimizing network-level travel time) subject to an environmental requirement. An example of environmental constraints is the link-based environmental capacity constraint, which defines a traffic flow limit that cannot be exceed because of the expected level of emissions that such an event would entail. This concept has been used in road pricing problems that consider fixed, variable, and uncertain travel demand (Ferrari, 1995; Yang and Bell, 1997; Li et al., 2012). Other types of environmental constraints are link-based emission constrains, which as their name suggest specifically constraint the level of emissions on roads (i.e., links) (e.g., see Nagurney, 2000), and network-wide emission constrains, which constraint the total level of emissions generated on the road network. The latter type of constraint is particularly relevant in the context of greenhouse gas emissions, which have global, but not local, effects in the short term (Sharma and Mishra 2013).

Environmental considerations can also be conceptualized as planning objectives that must be maximized or minimized. The most common environmentally-oriented planning objectives is the minimization of traffic emissions, which is sometimes accompanied by objectives related to travel conditions (i.e., a bi-objective design problem) (Yin and Lu, 2000; Yin and Lawphongpanich, 2006). Less common are NDPs that consider human exposure to traffic emissions and environmental equity. In the model proposed by Wang et al. (2014), a road pricing model is proposed that incorporates the objective of minimizing the pollutants inhaled by drivers, among other objectives. Rodriguez-Roman and Ritchie (2017) proposed an NDP where both total intake of pollutants and environmental inequality are minimized. In this model, total intake of pollutants and environmental inequality was measured using static distributions of populations surrounding the road network and the pollutant concentration levels at receptor points.

2.2 NDPs for the Design of ACP Schemes

Existing ACP design models for practical planning applications have focused on congestion pricing. Generally, in these problems the decision maker's objective is to select a charging cordon's location and tolling level that maximize the traveling public's social welfare, measured in terms of travel costs. The user equilibrium problem with elastic demand is utilized to model traffic changes due to candidate pricing

schemes. Zhang and Yang (2004) proposed the cordon-based congestion pricing problem and developed a genetic algorithm (GA) approach for its solution. This GA heuristic incorporates the graph theory concept of a cutset to test a cordon's feasibility (i.e., to ensure a closed cordon). Sumalee (2004) also developed a GA procedure for cordon pricing, but this algorithm employs a branch-tree framework to encode the network's charging boundary. In this version of the problem the cost of implementing a cordon pricing scheme is considered as part of the decision maker's objective. The GA-based heuristic proposed by Maruyama et al. (2014) departs from the previous graph-based frameworks by employing computational geometry concepts for the search of optimal cordon locations. Hult (2006) reports similar efforts by the UK Department of Transport (DoT) to use a GA-based geometrical approach for the cordon-based congestion pricing problem. In a study by Zhang and Sun (2013), the cordon problem was formulated as a mathematical program with complementarity constraints, and a dual-heuristic solution algorithm was proposed.

Given their focus on congestion, the reviewed models utilize an aggregate representation of travel behavior for a single design time period, with no consideration of how pricing affects individuals' activity participation, activity scheduling, and mode choice behaviors, or how ACP schemes impact the generation and dispersion of vehicle-generated air pollutants. In the next section, an environmentally-oriented ACP design model is presented, along with a methodology that incorporates models to simulate travelers' activity patterns, as well as their associated exposure to pollutants. In addition, new single- and multi-objective solution heuristics are proposed to solve ACP design problems.

Multi-objective considerations are important for the design of environmentally sustainable ACP schemes as the human health risks associated with the exposure to vehicle-generated pollutants depend on factors such as the quantity of emitted pollutants, the population densities at various times and distances from emission sources, and the variability of atmospheric conditions (Levy et al., 2010). Advancing ACP models beyond congestion-related objectives is also supported by theoretical studies that show that minimizing congestion does not necessarily lead to improved environmental conditions (Nagurney, 2000b), and that the design of sustainable cordon pricing schemes should account for traffic emissions (Li et al., 2014).

2.3 Applications of Surrogate-Based Optimization in Transportation Planning and Engineering

The practical application of optimization based-methods to ACP design problems is limited given the time-consuming nature of the models used to simulate the effects of an ACP scheme. This issue is compounded in the case of environmentally-oriented ACP design problems, as these problems require the modeling of vehicle emissions, pollutant concentrations, and, potentially, human exposure to pollutants. The increasing complexity of travel behavior and environmental impact assessment models require the development of efficient heuristics to solve optimization-based NDPs like the ACP problems. A promising solution approach is surrogate-based optimization. A surrogate model (also known as a metamodel or a response surface model) is a computationally inexpensive approximations to computationally expensive models. In surrogate-based optimization the surrogates are used to predict the value of time-consuming functions (i.e., models). On the basis of the surrogate predictions the heuristics screen for (or select) the candidate designs that are more promising. These selected solutions are then evaluated with the computationally expensive models. In transportation engineering applications, surrogate-based heuristics has been shown to accelerate the discovery of good solutions for continuous (e.g., Chow et al., 2010; Osorio and Bierlair, 2013; Lamotte, 2014; Chen et al., 2014), discrete (Xiong and Schneider 1992; Fiske 2011; Wismans, 2012) and mixed integer NDPs (Chen et al., 2015; Rodriguez-Roman and Ritchie 2017). This report presents a new set of surrogate-based heuristics designed to search for good solutions to ACP design problems.

2.4 Overview of ABMs

At the core of the proposed activity model lies an activity-based travel behavior model. Studies on such models date back to almost half a century ago, and have resulted in a wide spectrum of approaches, including utility-maximization models (Adler and Ben-Akiva, 1997; Brownstone and Small, 1989; Bhat et al., 2004; Kitamura et al., 2000; Pendyala et al., 2005), rule-based models (Arentze et al., 2000; Miller and Roorda, 2003; Auld and Mohammadian, 2012), and network-based models (Recker et al., 1989; Recker, 1995; Recker, 2001). In order to account for transportation demand elasticity, as reflected in changes in travel behavior and activity scheduling, we will use a network-based approach to infer scheduling behavior of travelers. This model advances the household activity pattern problem (HAPP) proposed by Recker (1995), a mixed integer programming (MIP) model analogous to the pick-up and delivery problem with time windows. In this model, it is assumed that individuals plan their daily activities such that generalized disutility is minimized. Several HAPP extensions have been developed and applied during the years. Gan and Recker (2008) expanded the HAPP model to handle uncertainties in travel time and activity duration that potentially lead to rescheduling (Chow and Recker, 2012; Allahviranloo and Recker, 2013; Allahviranloo and Recker, 2014; Regue et al., 2015). In this project, existing network- and activity-based models were extended by incorporating mode choice and variable travel time to HAPP. Two modes of transit and personal vehicles and three travel time matrixes (representing morning and afternoon peak hours and other times) were used in the analysis and application of the new model. Activities were divided into two categories of fixed and flexible, where flexible activities can be rescheduled or relocated to improve the associated utility gained from conducting a set of activities.

3 Methodology

This section describes the formulations of the ACP design problems, the model systems used to estimate the user response to an ACP scheme, and the proposed solutions heuristics.

3.1 General Problem Formulations

An optimization-based approach is proposed for the design of ACP schemes that account for both mobility and environmental goals. In general terms, the design problem is formulated as a bi-level, simulation-based optimization problem. The problem's upper-level consists of the decision maker's objectives, constraints, and decision variables. There are two decision variables: the location of the charging boundary and the associated tolling level. Users' travel response to the decision maker's decisions and the resulting system-wide impacts are modeled in the problem's lower-level.

Two general problem formulations are discussed next. In the first problem, a single planning objective is envisioned in conjunction with an environmental constraint (resulting in a single objective integer programming problem with constraints). In the second design problem, it is assumed that the decision-maker seeks a pricing scheme that optimizes an environmental objective and a mobility-related objective (that is, a bi-objective integer programming problem). The general problem formulations of these problems are followed by examples of specific planning objectives that could be used to design an ACP scheme.

The road network is represented using a graph (i.e., nodes and links). The optimal charging boundary and the associated tolling levels are denoted by \mathbf{y} and $\boldsymbol{\tau}$. \mathbf{y} denotes the set of tolled road segments that enclose the urban region targeted by the pricing scheme. Each element of \mathbf{y} indicates if a road segment (j) is part of the charging boundary ($y_j = 1$) or not ($y_j = 0$). Values of \mathbf{y} that create a closed charging boundary are said to be part of set θ , a set that, in addition, contains all boundaries that satisfy the shape constraints to be discussed in this section. $\boldsymbol{\tau}$ is a set that contains the toll level information at the link level. For simplicity, a single tolling level is considered, represented by τ . If a road segment j is part of the charging boundary then the toll τ is charged on the segment ($\tau_j = \tau$). It will be assumed that the agency defines a set of acceptable tolling levels, ranging from τ_{min} to τ_{max} . \mathbf{v} contains information on the system-wide response to the pricing scheme, as modeled by the lower-level models. For expositional clarity, referenced will be made in the discussion that follows to area pricing only. Note that the models and solution heuristics can be applied with equal ease to the design of cordon pricing schemes.

3.1.1 Single-Objective Area Pricing Problem

Consider a transportation agency that is interested in designing an area pricing scheme to reduce pollutant concentration levels at receptor points (C_r) below a regulatory threshold C_{max} (for simplicity, a single pollutant type is considered) while simultaneously minimizing a planning objective M related to travel conditions in the network (see Section 3.1.3 for possible specifications of M). The upper-level design problem can be formulated as:

$$\min_{\mathbf{y}, \boldsymbol{\tau}} M(\mathbf{y}, \boldsymbol{\tau}, \mathbf{v}(\mathbf{y}, \boldsymbol{\tau})) \quad (1)$$

subject to

$$C_r(\mathbf{y}, \boldsymbol{\tau}, \mathbf{v}(\mathbf{y}, \boldsymbol{\tau})) \leq C_{max} \quad \forall r \quad (1.1)$$

$$\boldsymbol{\tau} \in \{\tau_{min}, \dots, \tau_i, \dots, \tau_{max}\} \quad (1.2)$$

$$\tau_j = y_j \tau \quad \forall j \quad (1.3)$$

$$y_j \in \{0, 1\} \quad \forall j \quad (1.4)$$

$$\mathbf{y} \in \theta \quad (1.5)$$

Note that constraints 1.1 have a single threshold value C_{max} , which can be interpreted as a pollutant concentration limit established by an air quality regulatory agency. To simplify the problem, the constraints 1.1. can be substituted by:

$$\max_r [C_r(\mathbf{y}, \boldsymbol{\tau}, \mathbf{v}(\mathbf{y}, \boldsymbol{\tau}))] \leq C_{max} \quad (1.1b)$$

3.1.2 Bi-Objective Area Pricing Problem

In the bi-objective area pricing problem it is assumed that the decision-maker seeks a scheme that minimizes a travel related objective M and an environmental objective H . This problem is stated as:

$$\min_{\mathbf{y}, \boldsymbol{\tau}} F(\mathbf{y}, \boldsymbol{\tau}, \mathbf{v}) = \begin{cases} M(\mathbf{y}, \boldsymbol{\tau}, \mathbf{v}(\mathbf{y}, \boldsymbol{\tau})), \\ H(\mathbf{y}, \boldsymbol{\tau}, \mathbf{v}(\mathbf{y}, \boldsymbol{\tau})) \end{cases} \quad (2)$$

subject to

$$C_r(\mathbf{y}, \boldsymbol{\tau}, \mathbf{v}(\mathbf{y}, \boldsymbol{\tau})) \leq C_{max} \quad \forall r \quad (2.1)$$

$$\tau \in \{\tau_{min}, \dots, \tau_i, \dots, \tau_{max}\} \quad (2.2)$$

$$\tau_j = y_j \tau \quad \forall j \quad (2.3)$$

$$y_j \in \{0,1\} \quad \forall j \quad (2.4)$$

$$\mathbf{y} \in \theta \quad (2.5)$$

Like in Problem 1, constraints 2.1 can be substituted by constraint 1.1b. The next subsection provides examples of formulations for the M and H objectives.

3.1.3 Specification of Travel-Related Planning Objectives

The specifications of the planning objectives can depend on the type of models at the analyst's disposal. An easy-to-compute evaluation measure is the change in consumer surplus produced by the pricing scheme (de Jong et al., 2007). Consumer surplus is a common metric of benefit. This measure can be computed with the outputs of the discrete choice models commonly used in regional transportation planning models. Specifically, the change in consumer surplus can be computed using the logsum of the logit models used to simulate mode choice, destination choice, and/or departure time choice in planning models. Let G denote the number of population groups in the travel demand model, and ρ_g signify the population size of each group g . Each population group can be distinguished in terms of its area of residence and marginal utility of income α_g . Prior to the introduction of a pricing scheme, a person belonging to group g obtains V_{gj} utility from travel alternative j . Given a scheme specified by $(\mathbf{y}, \boldsymbol{\tau})$, the utility changes to $V_{gj}(\mathbf{y}, \boldsymbol{\tau}, \mathbf{v})$. Given this terminology, the objective of maximizing the change in consumer surplus is formulated as:

$$M^{CS}(\mathbf{y}, \boldsymbol{\tau}, \mathbf{v}) = \sum_t \sum_g \frac{\rho_{gt}}{\alpha_g} \left(\ln \left(\sum_j e^{V_{gjt}(\mathbf{y}, \boldsymbol{\tau}, \mathbf{v})} \right) - \ln \left(\sum_j e^{V_{gjt}} \right) \right) \quad (3)$$

The index t in equation 3 represents a time period t in the planning model.

From the perspective of the single objective problem where the only environmental goal is to satisfy an environmental constraint, another sensible travel-related objective is to find the travel scheme that affects current travel conditions the least. That is, the decision-maker would attempt to minimize deviations from the status quo. This is an attractive travel objective from a political standpoint, as pricing schemes are

generally met with oppositions from groups that identify with the drivers affected by the tolling. Let s_{wt} represent the auto mode share for origin-destination pair w and time period t prior to the pricing scheme, and $s_{wt}(\mathbf{y}, \boldsymbol{\tau})$ represent the auto mode share under charging scheme $(\mathbf{y}, \boldsymbol{\tau})$. The objective of minimizing deviation from the status quo can be expressed as:

$$M^{SQ}(\mathbf{y}, \boldsymbol{\tau}, \mathbf{v}) = \sum_t \sum_w |s_{wt}(\mathbf{y}, \boldsymbol{\tau}, \mathbf{v}) - s_{wt}|^\xi \quad (4)$$

The ξ parameter is set by the analyst; typical values include $\xi = 2$ and $\xi = 1$.

Another meaningful goal is to find the minimum revenue generating area pricing scheme that satisfies the environmental constraints. For example, using the road flows (x_{jt}) for a particular time period t , a proxy of the total revenue generated represent can be formulated as:

$$M^R(\mathbf{y}, \boldsymbol{\tau}, \mathbf{v}) = \sum_j \tau_j x_{jt}(\mathbf{y}, \boldsymbol{\tau}, \mathbf{v}) \quad (5)$$

Alternatively, the decision-maker might be interested in generating a target level of revenue R^{target} , in which case the design objective could be to minimize the deviation between the revenue target and the revenue generated by the pricing scheme. This objective can be stated as:

$$M^{R+}(\mathbf{y}, \boldsymbol{\tau}, \mathbf{v}) = (M^R(\mathbf{y}, \boldsymbol{\tau}, \mathbf{v}) - R^{target})^2 \quad (6)$$

3.1.4 Specification of Environmentally-Oriented Planning Objectives

This work focuses on the effects of vehicle-generated air pollutants on the environment, and in particular on the detrimental human health outcomes caused by polluted environments. Note, however, that there are other types of pollution by-products of transportation activities, such as sound pollution. Additionally, given the public health dimension of this research, the models focus on emission and concentration of pollutants that have local effects, as opposed to the total emission of pollutants that have long-term, global effects (e.g., CO₂).

Yet, total emission measures can be a useful, albeit imperfect, proxy to the public health effects of vehicle-generated emissions. An average speed approach to computing link-level emissions is common in practice, especially in the context of regional analyses that depend on the outputs of static traffic assignment models. Let e_j represent an emission factor (in units of grams of pollutants per unit of distance per vehicle) that is computed as function of the average speed on a link j of length l_j , and let x_j represent the vehicle flow on that link (which in turn is a factor that determines the average speed). Given this setup, total network emissions are computed by:

$$H^E(\mathbf{y}, \boldsymbol{\tau}, \mathbf{v}) = \sum_j l_j e_j(x_j) x_j(\mathbf{y}, \boldsymbol{\tau}, \mathbf{v}) \quad (7)$$

A more direct proxy of health impacts of traffic emissions are pollutant exposure measures at the population level. In this type of measure, the level of exposure is assessed using average pollutant concentration levels C_r (estimated at a point in time in the zones that constitute the study area) and the number of people linked to each zone r (e.g., present in zone in the period). One alternative is using the population-level intake of vehicle emitted pollutants as a health impact proxy. Define B_g as the breathing rate of group ρ_g and C_{gr} as the pollutant concentration level to which members of group g in zone r are exposed to during the period of analysis. The population-level pollutant intake can be estimated using:

$$H^I(\mathbf{y}, \boldsymbol{\tau}, \mathbf{v}) = \sum_g \sum_r \rho_{gr} B_g C_{gr}(\mathbf{y}, \boldsymbol{\tau}, \mathbf{v}) \quad (8)$$

Note that pollutant intake can also be estimated at the agent-level (I_z). For this computation the analyst would need to estimate the time-space path that each agent follows throughout the day, as well as the pollutant concentrations encountered by the agent.

Specific estimates of health impacts extend the preceding analysis by mapping exposure to a health response. For example, linear exposure-response functions can be used to estimate the years of life lost (YOLL) as a function of an exposure to particulate matter (PM_{2.5}) (Rabl et al., 2014). Representing the slope of the linear exposure-response function as S_n (units: YOLL/(person in group $n \times \text{year} \times \mu\text{g PM}_{2.5}/\text{m}^3$)) and the value of life as VL (units: \$/YOLL), the health impact objective can be defined as:

$$H^L(\mathbf{y}, \boldsymbol{\tau}, \mathbf{v}) = VL \sum_n S_n \left(\sum_r \rho_{nr} C_{nr}(\mathbf{y}, \boldsymbol{\tau}, \mathbf{v}) \right) \quad (9)$$

The previous objectives are examples of measures of global efficiency; they are efficient from a utilitarian perspective in which the correct course of action is the one that results in the maximum benefit to society at large. An alternative perspective in environmentally-oriented planning is to ensure that there is an equitable distribution of benefits and costs for a given network intervention (e.g., a pricing scheme). In this study, environmental equity is considered in terms of the differences in pollutant exposure levels at the level of the individual. Following Levy et al. (2010), the level of inequality in pollutant exposure level can be quantified using the Atkinson index:

$$H^A(\mathbf{y}, \boldsymbol{\tau}, \mathbf{v}) = 1 - \left[\frac{1}{Z} \sum_{z=1}^Z \left(\frac{I_z(\mathbf{y}, \boldsymbol{\tau}, \mathbf{v})}{\bar{I}(\mathbf{y}, \boldsymbol{\tau}, \mathbf{v})} \right)^{1-\varepsilon} \right]^{\frac{1}{1-\varepsilon}} \quad (10)$$

where Z is the total number of agents, \bar{I} is the average pollutant intake, and ε is the Atkinson inequality aversion factor. At its extreme values, an H^A equal to zero signifies complete equality in exposure levels, while an H^A equal to one implies complete inequality.

3.2 Lower-Level Model System

Transportation analysts have several alternatives to model the travel response \mathbf{v} to pricing schemes, a response which could include changes in travel mode, routes, departure times, and activity participation and scheduling. This subsection discusses the basic features of the type of model systems necessary in the design of environmentally-oriented ACP schemes. In addition, the formulation of an activity-based travel demand model, tailored to this study, is presented, as well as a detailed description of the pollutant exposure model used in the project.

3.2.1 Features of Lower Level Model System

The public health effects of vehicle-generated pollutants strongly depend on the environment in which these pollutants are emitted and on the activity and travel behavior patterns of the population. Therefore, ideally, the response \mathbf{v} to a pricing scheme ($\mathbf{y}, \boldsymbol{\tau}$) would be generated via an activity-based model (ABM), as it would produce the travel tours needed to quantify the level of exposure to pollutants in the population. The components of an activity-based model system for the analysis of ACP schemes is shown in Figure 1. In this model system, a series of activity patterns serve as inputs to an ABM that simulates the activity

participation and scheduling behavior of agents, as well as their mode choice. The agent-level trips are aggregated to the zonal level and then loaded to a traffic assignment model that assigns the travel flows to the transportation network. The network flows are then used to compute the traffic emissions, followed by the application of a pollutant concentration model to simulate the concentration of pollutants in the microenvironments encountered or occupied by the agents. Lastly, given the pollutant concentration levels and the agent travel tours, an estimate of the human exposure to pollutants is produced, which could in turn be converted into an estimate of the health costs (e.g., in terms of YOLL) associated with vehicle emissions.

Note that in the model system proposed in Figure 1 the ABM model is linked to a static traffic assignment model, a common linkage that reduces the run time of the model system relative to model systems that link ABM models with dynamic traffic assignment models (Castiglione et al., 2015). Given the aggregate output of the static assignment models, the emission and air dispersion models used to compute pollutant concentrations are also specified as static.

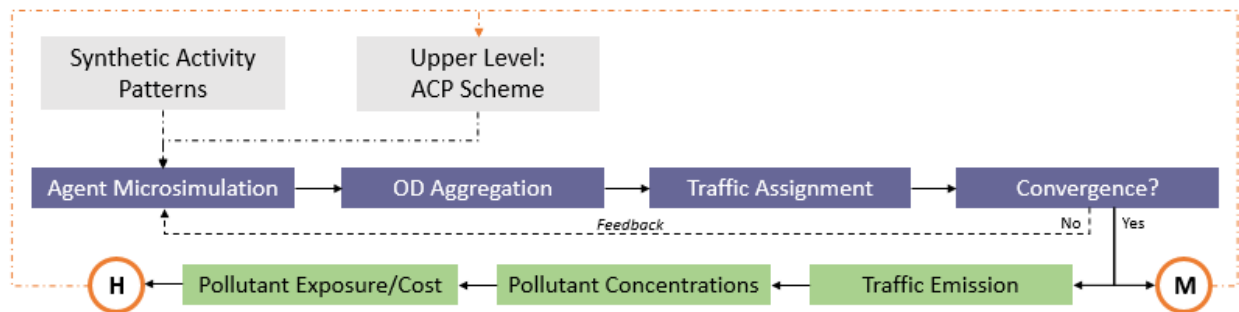


Figure 1. Lower-level model system

Even with a static assignment model, simulating the activity participation and scheduling patterns of millions of agents for a large metropolitan region could be time-consuming in the context of an optimization problem. For this type of situation, a second type of model system is presented in Figure 2 that can be used to analyze the effects of ACP schemes. In this case, a standard sequential planning model (e.g., the four-step model) supplants the ABM in the process of predicting travel demand and estimating the travel flows in the network. The travel time and cost outputs of the sequential planning model then serves as input to an ABM that simulates the activity participation and scheduling behavior of a sample of agents (in contrast to the total population of the region). The travel and activity schedule of the agents, in conjunction with the predicted pollutant concentrations, are then used to compute a sample-based measure of the pollutant exposure experienced by people in the community

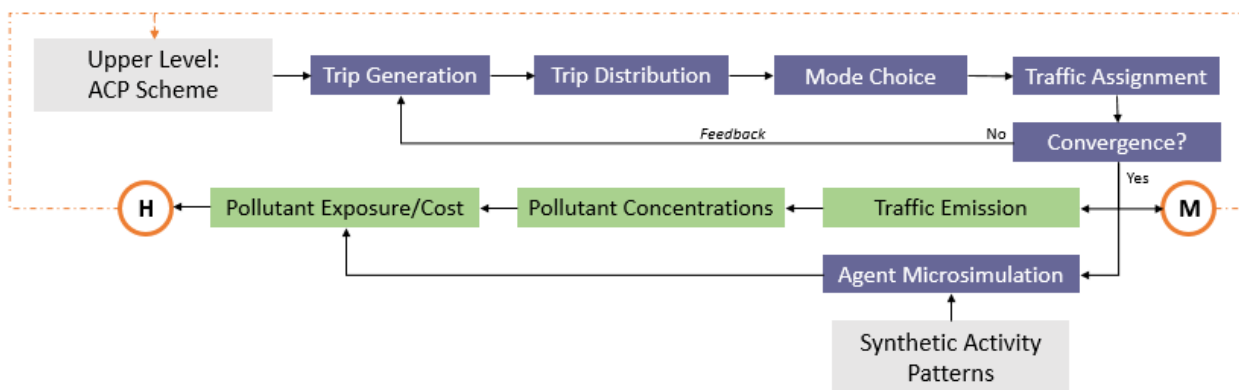


Figure 2. Simplified lower-level model system

Note that the two model systems presented so far are applicable to the bi-objective problem that considers and environmentally-oriented objective H that depends on the outputs of ABMs. For the single-

objective problem (Problem 1) where pollutant concentrations are the only concern environmental concern, the ABM and its related components would be removed from the lower-level model system.

3.2.2 The Household Activity Pattern Problem

The Household Activity Pattern Problem (HAPP) was used in this project as the framework to analyze the activity engagement behavior of the population, where activities are scheduled and planned using a network-based model. HAPP is a pick-up and delivery problem with time windows. In its context, each activity is considered as an object which needs to be executed (pick-up) at a location at a certain time and the person, after finishing each activity, may return to home (drop off) and then depart for the next activity location. In its original form, HAPP covers only one mode of transportation and it also uses one travel time matrix in its network modeling. In this project, one of the main objectives of the research is to evaluate the impacts of pricing on mobility behavior, as well as the overall performance of the policy in mitigating the externalities caused by traffic. To address this objective two changes were made to the HAPP. First, transit mode was integrated into the formulation, and second, different travel time matrixes to model behavior at different periods of the day were incorporated in the model. The HAPP objective function was set to minimize the total disutility of travel, defined as a combination of travel cost and travel time, and to minimize the deviation of the new activity itinerary for the original one that the person has performed according to the observed pattern. Activities are categorized into two sets: ‘flexible’ and ‘fixed’ sets of activities. Fixed activities, such as attending school or going to work, have a fixed location to be executed and are assumed to have fixed schedule (duration, start time, and end time). The flexible activities can be modified depending on the travel time matrix and the cost of travel to the location of the activity. Individuals can cancel, reschedule and relocate the activity. As an example, a trip to the grocery store during the day which would incur in a toll can be substituted by a stop in another grocery store outside of the tolled area or it can be performed in the evening when the pricing is inactive. Figure 3 depicts the possible changes that agents might apply to their travel agendas in response to the pricing policy.

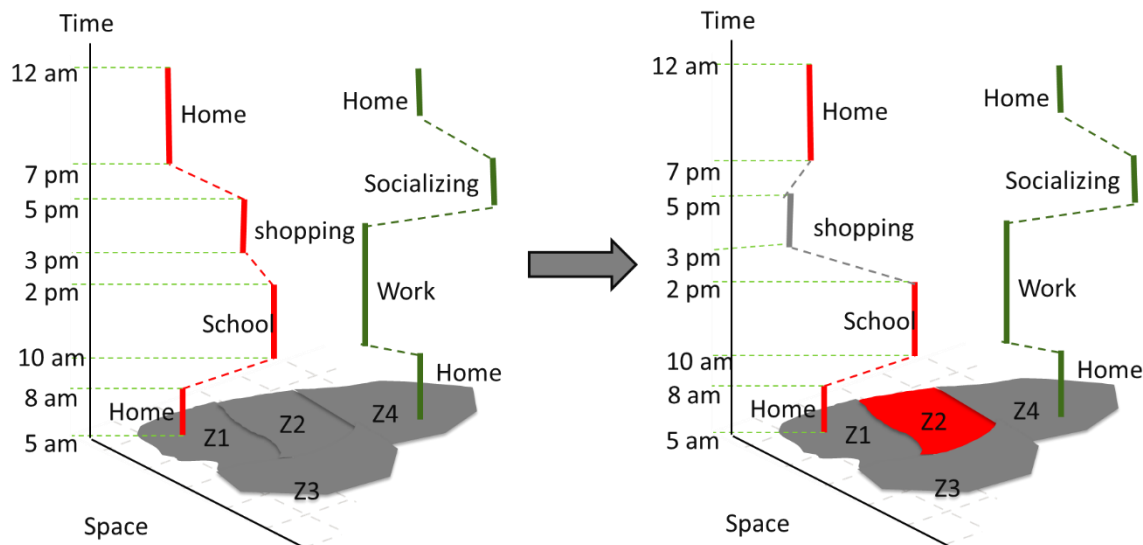


Figure 3. Example of activity pattern. Presents activity plan of 2 persons in the dimension of time and space. Person 1 relocates his shopping activity to another place once zone 2 is defined a cordon area

3.2.2.1 HAPP Formulation

The objective function of the core HAPP model consists of two terms: (i) minimizing the total travel cost and travel time and (ii) minimizing the deviation from the observed schedule and itinerary of the traveler. The proposed model is subject to the following constraints:

- *Vehicle routing constraints:*

Meaning that each fixed activity should be performed in its location by either of the modes that results in the highest utility. Also, each trip destined to a location by a specific mode has a corresponding trip departing from the same location with the same mode (conservation law). For flexible activities this constrained is relaxed since the activity has the cancelation option.

- *Time windows constraints:*

These are a set of equations mandating the opening hours and closing hours of the activities and the time associated with the activity start time and sequencing. For instance, attendance to school cannot start outside school hours. Additionally, if an activity is followed by another activity, the second activity cannot start prior to the end of the first activity and the time required to travel from the location of first activity to the second one.

In order to take into account the impacts of different modes of transportation and peak hour, the following set of equations are included in the model. It is assumed that the variations in the travel time can be summarized by three travel time matrixes: morning peak hour, afternoon peak hour, and non-peak hours. Therefore, three time slices are defined in this study. These time slices are defined by variable sc . $\lambda_{i,sc}^{vh}$ is a binary variable which takes the value of 1 if the trip using mode h serving node i in time slice sc , and zero otherwise. Assuming T represents arrival time to each location, $\lambda_{i,sc}^h$ is related to T_i^h through $\gamma_{i,sc}^h$, which is a real variable in the range of $[0,1]$ and is bounded by $\lambda_{i,sc}^h$ and $\lambda_{i,sc-1}^h$ as described in equation 11.2. b_{sc} refers to the vector of time slice boundaries. Say if the morning rush period is from 7 to 9 and evening peak period is from 16 to 18, then the elements of vector b are $[0,7,9,16,18,24]$. The HAPP formulation is then extended with the following constraints.

$$\sum_h \sum_{sc} b_{sc} \times \gamma_{i,sc}^h = T_i^h, \forall i \in N \quad (11.1)$$

$$\gamma_{i,sc}^h \leq \lambda_{i,sc}^h + \lambda_{i,sc-1}^h, \forall i \in N, sc \in \Lambda \quad (11.2)$$

$$\sum_{sc} \gamma_{i,sc}^h = 1, \forall i \in N \quad (11.3)$$

$$\sum_{sc} \lambda_{i,sc}^h = 1, \forall i \in N \quad (11.4)$$

$$t_{uw}^{vh} t_{i,j}^{vh} = \sum_{\tau \in \Lambda} \gamma_{i,sc}^{vh} \cdot (t_{i,j}^{vh})_{sc} \quad (11.5)$$

$$0 \leq \gamma_{i,sc}^h \leq 1 \quad (11.6)$$

$$\lambda_{sc,i} \in \{0,1\}, T_{i,u} \geq 0 \quad (11.7)$$

3.2.3 Modeling Human Exposure to Pollutants

The tours generated by the ABM enables the estimation of pollutant exposure at the individual-level (as opposed to the population-level). An agent z 's intake of air pollutants I_z during a day depends on the activities undertaken by the agent, the duration of the activity, and the pollutant concentration encountered in each location, among other factors. Intake I_z can be disaggregated into the agent's pollutant intake while stationary at a location (\dot{I}_z) (e.g., home, office) and the agent's pollutant intake while moving from one location to another (\tilde{I}_z) (e.g., going from home to work). I_z is computed as:

$$I_z = \dot{I}_z + \tilde{I}_z \quad (12)$$

Let m be a microenvironment visited by person z for a duration δ_{zm} . The concentration at m can be computed as $C_{omt} + f_m \times C_{mt}$, where C_{omt} represents the indoor pollution levels at m and time t , and f_m is a pollutant infiltration factor that maps the outdoor concentration C_{mt} to an indoor concentration. For simplicity, the term C_{omt} is set to zero in this project. Assuming a constant breathing rate B_z throughout the day, \dot{I}_z is the sum of the pollutants inhaled by the agents in all microenvironments visited:

$$\dot{I}_z = B_z \sum_m \delta_{zm} \times f_m \times C_{mt} \quad (13)$$

The agents' travel paths and modes used in those paths are required to compute the value of \tilde{I}_z . Assume that an agent's path q via mode h can be decomposed into a series of links j , each link with average pollutant concentration C_{jt} at time period t . The average travel time on link j is computed by l_j/v_j , where v_j is the average travel speed on link j . Given this notation, the agent's pollutant intake in path q via mode h can be estimated by:

$$\tilde{I}_{zhq} = B_z \sum_j \frac{l_j}{v_j} \times f_{hj} \times C_{jt} \quad (14)$$

f_{hj} is the pollutant infiltration factor for the mode h in link j . \tilde{I}_z is estimated by adding all paths' \tilde{I}_{zhq} :

$$\tilde{I}_z = \sum_h \sum_q \tilde{I}_{zhq} \quad (15)$$

3.3 Heuristics for Solving Area Pricing Problems

The formulations of a single- and bi-objective ACP design problems were presented in Section 3.1. As discussed in Section 2.2, there are at least five heuristics in the literature to solve single-objective ACP design problems. In this section, two new surrogate-based solution heuristics (SBSH) are proposed: one for the single-objective problem and the other for the bi-objective problem, which could generally be used for multi-objective problems. Both heuristics employ surrogate-based optimization techniques, use a geometric representation of the charging boundary, and control for the final shape of the charging boundary. This section is divided into four main subsections. The first two subsections explain how the surrogate models are fitted and used, and how the charging boundaries are represented. The last two subsections describe the two solution heuristics.

3.3.1 Fitting and Using Surrogate Models

As previously mentioned, a surrogate model is a function that can be quickly evaluated by a computer to produce an approximation to a model that takes considerable time to run. The computationally expensive model takes as input a set of variables \mathbf{X} and it produces an output Y . Generally, the surrogate models would also take as input a set of variables \mathbf{X} (or a subset or product of those variables) to produce an estimate \hat{Y} of the output of the computationally expensive model. In the context of this work, the variables \mathbf{X} would represent the features that define the charging scheme (i.e., the boundary and toll), and the output Y could be the value of a planning objective function or pollutant concentration constraint function, both of which require computationally expensive computer models for their evaluation. As it will be shown in the next sections, the proposed heuristics screen for the best designs from a pool of thousands of candidates based on the surrogate model predictions for each candidate.

An initial set of runs of the computationally expensive models is needed to fit the surrogates. That is, an initial set of designs $\{\mathbf{X}_1, \mathbf{X}_2, \dots, \mathbf{X}_{n_0}\}$ is evaluated via the time-consuming models to produce a set of outputs $\{Y_1, Y_2, \dots, Y_{n_0}\}$. Then the surrogate models are fitted using the (\mathbf{X}, Y) pairs as data samples; \mathbf{X} are the independent variables used to predict the dependent variable Y . As the heuristics select new designs and evaluate them via the computationally expensive models, new (\mathbf{X}, Y) pairs are generated and the surrogate models are updated. Naturally, the procedures used to fit the surrogate models will depend on the type of surrogate model used. Commonly used surrogate model types include polynomial regression models, radial basis functions, and kriging (see Forester and Keane, 2009). Any of these and other surrogate model types can be employed in the heuristics presented next.

3.3.2 Representing the Charging Area

In this study charging areas are represented using geometric shapes. Zones that are within the space enclosed by a geometric shape are part of the charging area, while those that are outside the shape are not part of the area. A geometric representation is used as it can, relative to other types of representation, represent complex boundary shapes with minimal information. As the location of the boundary is a decision variable, the way this information is encoded determines how many initial candidate charging schemes (i.e., design solutions) need to be evaluated with the computational costly models prior to estimating useful surrogate models. As previously discussed, a surrogate model s is fitted using the information of a set of (\mathbf{y}^n, τ^n) solutions (i.e., $\mathbf{X}^n = (\mathbf{y}^n, \tau^n)$) as independent variables, and an output of the computationally expensive models (e.g., $Y^n = M^n(\mathbf{y}^n, \tau^n)$) as dependent variable. So, besides creating a harder optimization problem to solve, more decision variables mean more computational time before the surrogate models can be estimated or, more fundamentally, before they can be used to provide accurate function predictions (as in any data-based prediction model, more data results in a better trained surrogate model). Hence the need for data efficient representations of charging boundaries in the context of surrogate-based optimization.

The drawback of geometric representation is that it is possible for different shapes to contain the same zones, and therefore represent the same charging area. For this reason, in the proposed algorithm the geometric shapes are mapped into the charging area representation proposed by Zhang and Yang (2004). In their algorithm, the charging area is represented by a binary vector $\boldsymbol{\eta}$ of length equal to the number of graph nodes that can be within the charging area. Each element of $\boldsymbol{\eta}$ is a binary variable that indicates if a node is in the charging area. $\boldsymbol{\eta}$ is used to define which network links must be tolled. Besides being useful for determining the uniqueness of the geometric shapes used in the SBSH, $\boldsymbol{\eta}$ is used, along with the cut-set concept, to determine whether the geometric shape forms a closed boundary. The $\boldsymbol{\eta}$ representation could technically be used directly to estimate surrogate models (i.e., $s(\boldsymbol{\eta}, \boldsymbol{\tau})$). However, the relatively large number of decision variables resulting from the $\boldsymbol{\eta}$ representation (including the toll, $|\boldsymbol{\eta}| + 1$ variables)

would likely make the estimation and use of surrogate models an impractical task, for the reasons previously discussed.

Here the charging area boundaries are represented using simple polygons, which are defined by an ordered collection of p vertices (see Figure 4). Let $\mathbf{P} = \{(r_i, \theta_i): i = 1, \dots, p\}$ represent the collection of vertices that define a charging boundary, where r_i and θ_i are the polar coordinates of the vertex i relative to a reference point O that is treated as the anchor of the charging area. Other types of geometric shapes could be used, but simple polygons are attractive because they are economical; the polygon is completely specified by the vertices without the need for additional parameters. Associated to each polygon boundary are $2p + 1$ decision variables (the vertex coordinates and the toll).

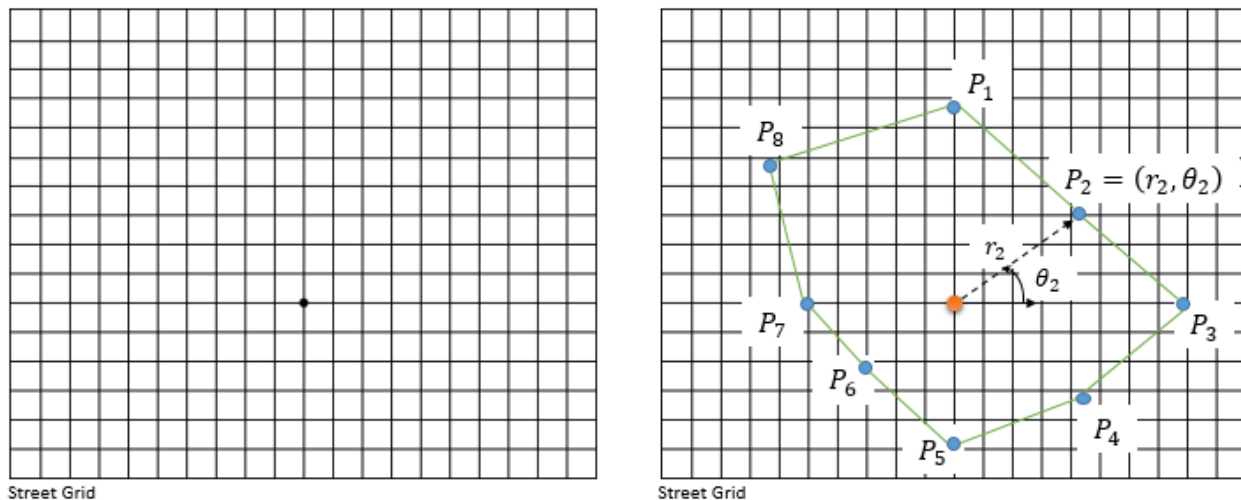


Figure 4. Simple polygon representation of charging boundary

Note that in the proposed algorithm, \mathbf{P} maps to $\boldsymbol{\eta}$ and $\boldsymbol{\eta}$ maps to \mathbf{y} . It is the polygon and toll information, however, that is used to predict the objective function and the concentration constraint values. For example, the expected mobility objective value \hat{M} of a candidate solution k is predicted using $\hat{M} = s^M(\mathbf{P}^k, \tau^k)$, where the surrogate model s^M is trained using previously evaluated $(\mathbf{P}^0, \tau^0, M^0)$ data points.

3.3.3 SBSH for Single-Objective Area Pricing Design Problems

The SBSH for the single-objective design problem (SBSH-SP) follows the general logic of the metric stochastic response surface algorithms proposed by Regis and Shoemaker (2007). An initial population of n polygons and tolls is generated and evaluated with the computationally expensive models. The resulting data points $\{(\mathbf{P}_j, \tau_j, M_j)\}$ are used to estimate the surrogate model s . In each iteration, five groups of candidate points are generated according to different set of rules (explained in the next section), and, among thousands of candidates, a candidate is selected for each group. This selection is partly made based on the surrogate model's prediction of each candidate's objective function value. The surrogate model s is updated after each iteration as new information (i.e., new data points $(\mathbf{P}_j, \tau_j, M_j)$) is learned.

The next subsections describe: (a) the constraint handling procedures used in SBSH-SP, (b) the criteria used to select the most promising candidate solutions, (c) the strategies used to generate the candidate solutions, and (d) the steps of the heuristics.

3.3.3.1 Constraint Handling Methods

Two versions of the SBSH-SP are proposed. These versions differ in the way that they handle the pollutant concentration constraint. The first version employs a penalty approach (Deb, 2000). From the minimization

perspective, let F_{max} be the objective function value of the worst known feasible solution, and κ be a penalty factor. Problem 1's objective function is restated (arguments omitted) as:

$$\tilde{F} = \begin{cases} F & \text{if } C_r \leq C_{max} \quad \forall r \\ F_{max} + \kappa \times \left(\max_r(C_r) - C_{max} \right) & \text{otherwise} \end{cases} \quad (16)$$

where F represent the objective function value (e.g., the M function in Problem 1). F_{max} is updated as worse feasible solutions are discovered. If there is no known feasible solution (an unlikely occurrence if a high enough toll is contemplated as an option), a placeholder value is assumed for F_{max} . This version of the SBSH-SP is identified as SBSH-SP-P.

The second version of the SBSH-SP handles constraint by using a surrogate model s^C to predict the value of function:

$$\tilde{c}_{max} = \max_r(C_r) \quad (17)$$

The maximum pollutant concentration level of a candidate design is predicted using surrogate s^C ; if the prediction is greater than C_{max} , then the candidate is removed as it is likely to be an infeasible solution. This version of the SBSH-SP is identified as SBSH-SP-S.

3.3.3.2 Selection Criteria for Identifying Most Promising Solutions

In each iteration of the SBSH-SP a set of candidate solutions is generated according to five sets of rules (i.e., five groups of candidate solutions are generated). In each group, each candidate is given a score W that is computed based on its predicted objective function value (surrogate score U^{RS}), a measure of each candidate's distance to previously evaluated points (distance score U^D), and weights w^{RS} and w^D corresponding to these two criterions ($w^{RS} + w^D = 1$). The score is computed by $W = w^{RS}U^{RS} + w^DU^D$. The candidates with the lowest W score are selected. For a candidate scheme (\mathbf{P}^k, τ^k) , the score $U^{RS,k}(\mathbf{P}^k, \tau^k)$ is computed using:

$$U^{RS,k}(\mathbf{P}^k, \tau^k) = \frac{s(\mathbf{P}^k, \tau^k) - s_{min}}{s_{max} - s_{min}} \quad (18)$$

where s_{min} and s_{max} are the minimum and maximum predicted objective function values, respectively, among the candidate solutions of each group. If s_{min} and s_{max} are equal, then $U^{RS}(\mathbf{P}^k, \tau^k) = 1$.

The purpose of the distance criterion score U^D is to measure how different a candidate solution is from previously evaluated solutions. Given that multiple polygons can result in the same charging zone (in terms of which nodes are within the charging area), the distance criterion is computed using the $\boldsymbol{\eta}$ mapping of each polygon. The minimum distance $\Delta(\boldsymbol{\eta}^k, \tau^k)$ between candidate $(\boldsymbol{\eta}^k, \tau^k)$ and the previously n evaluated schemes is computed along with the related minimum ($\Delta_{min} = \min_{1 \leq k \leq n} \{\Delta(\boldsymbol{\eta}^k, \tau^k)\}$) and maximum ($\Delta_{max} = \max_{1 \leq k \leq n} \{\Delta(\boldsymbol{\eta}^k, \tau^k)\}$) distances. Score $U^{D,k}(\boldsymbol{\eta}^k, \tau^k)$ is calculated using:

$$V^D(\boldsymbol{\eta}^k, \tau^k) = \frac{\Delta_{max} - \Delta(\boldsymbol{\eta}^k, \tau^k)}{\Delta_{max} - \Delta_{min}} \quad (19)$$

Again, if Δ_{min} equals Δ_{max} , then $V_n^{dist}(\boldsymbol{\tau}^m) = 1$. The weight of each criterion (w^{RS} and w^D) is cyclically adjusted in each iteration. For this purpose, an ordered set $Y = \langle v_1, \dots, v_k \rangle$ ($0 \leq v_1 \leq \dots \leq v_k \leq 1$) is

defined; with each iteration w^{RS} is sequentially assigned a value from Y . The purpose of adjusting the weights in this manner is to alternate between exploitative and explorative search.

The selected solutions are evaluated with the computationally expensive models. The information of the evaluated candidates is stored in data archives that are used to re-estimate the surrogate model at the start of each iteration, as previously mentioned. An additional data archive is used to store the best known charging area scheme (i.e., the feasible solution with lowest objective function value). This best-known solution is used in the generation of candidates.

3.3.3.3 Procedures to Generate Candidate Solutions in SBSH-SP

Five candidate solution groups are generated in each iteration of SHSB-SP. The first three candidate groups are created using information from the best known charging area boundary $\mathbf{P}^{best} = \{\mathbf{r}^{best}, \boldsymbol{\theta}^{best}\}$. The first group of candidates (type I) share the boundary \mathbf{P}^{best} , but differ in their toll level τ^k . The number of type I candidates, D^I , depends on how many of \mathbf{P}^{best} possible toll values have been evaluated. In the unlikely case that all tolls are evaluated for \mathbf{P}^{best} , the analyst could decide to simply stop producing type I candidates or switch the \mathbf{P}^{best} information with data from another feasible solution (e.g., the second best known solution). In the heuristic implemented for the numerical tests, a reduced toll set was generated in the interval $[\tau^{best} - \varepsilon, \tau^{best} + \varepsilon]$, and the most promising toll was selected from this set.

In the second group of candidates (type II), D^{II} charging area boundaries are generated adjusting the \mathbf{P}^{best} boundary while keeping the radii and toll level fixed. Three strategies are used to adjust the radii: expansion, contraction, or expansion and contraction. With probability Γ^U , the expansions are made uniformly according to $r_j^{k,II} = (1 + \omega) \times r_j^{best}$, where ω is a randomly generated number obtained from the interval $[\omega^{min}, \omega^{max}]$. Similarly, in boundary contractions the radii are uniformly adjusted using $r_j^{k,II} = (1 - \omega) \times r_j^{best}$ with probability Γ^U . For expansion and contraction candidates a radius j is selected and the radii before j are uniformly expanded while the radii from j are contracted, or vice versa (with equal probability). With probability $1 - \Gamma^U$, the same procedure as the one previously described is applied, but with distinct ω factors (i.e., non-uniform expansion, contraction, or contraction and expansion with individual ω_j random number). For the expansion and contraction candidates, the radii are adjusted using $r_j^{k,II} = r_j^{best}(1 + b\omega_j)$, where b is a random variable that can assume the values of -1 and 1 with equal probability. The heuristic keeps track of the adjustment strategy used in each iteration. When a candidate is found that is better than the current \mathbf{P}^{best} , the next iteration uses the same strategy that resulted in the successful candidate. For example, if the current \mathbf{P}^{best} was bested by an expansion candidate, the next type II candidates will be generated using an expansion adjustment (the boundary will keep expanding).

The radii and the angles are adjusted in the third group of candidate solutions (type III). Two radii adjustment modalities are utilized: coordinated and uncoordinated adjustments. The uncoordinated radii adjustments use the same formulas as the ones discussed for type II candidates. In the coordinated operations the radii perturbations are coordinated around a randomly selected focal vertex j . Vertex j is assigned the largest radius length perturbation $\Delta = \omega d^{max}$, where d^{max} is the maximum vertex displacement allowed. In a controlled expansion, vertex j is moved by $r_j^{k,III} = r_j^{best} + \Delta$, and in a contraction by $r_j^{k,III} = r_j^{best} - \Delta$. The neighboring vertices ($j - 1$ and $j + 1$) are perturbed by a percent δ of Δ . The percent δ_{j+1} (or δ_{j-1}) is computed recursively using $\max(0, \delta_j - \omega^\delta)$, where ω^δ is a randomly generated number in the interval $[\omega^{\delta,min}, \omega^{\delta,max}]$ and the initial δ_j is set to 1. The percent for $j + 2$ is $\max(0, \delta_{j+1} - \omega^\delta)$, and so on. Then, the controlled expansion for vertex $i \neq j$ is $r_i^{k,III} = r_i^{best} + \delta_i \Delta$ and the controlled contraction $r_i^{k,III} = r_i^{best} - \delta_i \Delta$. For controlled expansion and contraction operations two focal points are selected, one for expansion and one for contraction, and the previous procedure is followed. Vertex radii are expanded or contracted according to the closest focal point (in the vertex sequence, not spatially). The vertex equidistant to the expansion and contraction focal points is perturbed by taking an

average of the contraction and expansion perturbations. For all operations, D^{III} boundaries are generated, half of which are produced using the coordinated adjustment procedures, and the other half using the uncoordinated procedures. Each type III boundary is replicated $|\tau|$ and assigned a unique toll level from the set $\tau = \{\tau_{min}, \dots, \tau_{max}\}$. In both coordinated and uncoordinated operations, the vertex angle $\theta_j^{k,III}$ is generate with the formula $\theta_j^{m,III} = \theta_j^{best} + \varphi$, where φ is a random number drawn from a normal distribution with zero mean and variance σ^2 .

The fourth set of candidates are generated using GA operators. D^{IV} candidates are generated by selecting two parents from the pool of evaluated solutions. With equal probability, a one-point or two-point crossover operation is performed with the parent's vertex information. Four strategies are applied for the one-point crossover modality: a) the same crossover point (i.e., vertex) is applied to swap the radii and angle information between the parents, b) one crossover point is used to swap the radii information and a different point is used to swap the angles, c) the one-point crossover swap is performed only for the radii, or d) the one-point crossover swap is performed only for the angles. With equal probability, one of these strategies was used to generate each of the D^{IV} candidates. With probability Γ^{mut} , a radii was mutated by applying either an expansion or a contraction factor as discussed for type II candidates. For the two-point crossover operations the same steps are followed, with the added detail that two crossover points are selected. Like in the case of type III solutions, each type IV boundary is replicated $|\tau|$ times and assigned a unique toll from the set $\tau = \{\tau_{min}, \dots, \tau_{max}\}$. A distinct set Y^{GA} was used to weigh the criterions used to select the most promising solution from the type IV candidates.

The last group of candidates is randomly generated. An anchoring radii length is r^{mV} is generated in the interval $[r^{min}, r^{max}]$. Then each radius is set according to $r_j^{mV} = r^{mV}(1 + b\omega_j)$. The angles are initially set so that the vertices are equidistant (resulting in an ordered sequence $\{\theta_1^V, \dots, \theta_j^V, \dots, \theta_p^V\}$), and then each angle is perturbed using $\theta_j^{m,V} = \theta_j^V + \varphi$. Once again, the M^V boundaries are replicated $|\tau|$ times and assigned a unique toll from the set $\tau = \{\tau_{min}, \dots, \tau_{max}\}$.

Note that the rules that define IV and V candidates are meant to prevent the algorithm from being trapped in a particular $(\mathbf{P}^{best}, \tau^{best})$ solution. As another safeguard against this potential problem, the heuristic keeps track of the number of candidate evaluations performed via a computationally expensive models without an improvement upon $(\mathbf{P}^{best}, \tau^{best})$ (i.e., the number of failures, stored in counter G_{fail}). If the number of failures exceeds a threshold $G_{max, fail}$, $(\mathbf{P}^{best}, \tau^{best})$ is supplanted in groups I, II, and III, by the next best solution that does not share the \mathbf{P}^{best} boundary, and the failure counter G_{fail} is reset to zero. Also, G_{fail} is reset when a candidate solution is discovered that bests $(\mathbf{P}^{best}, \tau^{best})$ solution. The objective of this procedure is to continually move the focus of the type I, II, and III procedures away from exploring a solution space that is not yielding superior solutions.

Before a candidate k is given a score W , it must pass five feasibility checks. The polygon \mathbf{P}^k must be a simple polygon (i.e., composed of non-intersecting line segments), as intersecting polygons generally have no practical meaning. If the polygon is simple, it is then checked that its transformation to $\boldsymbol{\eta}^k$, along with its toll τ^k , have not been previously evaluated. Additionally, the $\boldsymbol{\eta}^k$ transformation must meet the cutset criterion used by Zhang and Yang (2004), which ensures that the polygon creates a closed boundary. The polygon shape must also meet the convexity criterion (Maruyama et al., 2014), and, the angle between three contiguous polygon vertices $(j - 1, j, j + 1)$ must not be less than ϱ . The last three conditions are the shape constraints that define the requirements for set θ (in constraints 1.5 and 2.5). In the case of SBSH-SP-S, the candidates that are predicted to be infeasible by the surrogate s^C are also eliminated.

3.3.3.4 SBSH-SP steps

The algorithm steps and the notation used in the description of SBSH-SP are presented next.

Decision variables

- τ : charging zone toll level
 \mathbf{P} : vertices defining changing zone boundary

Indices

- k : indices for candidate solution vectors generated according to the rules of groups I through V
 u : indices for the five candidate solutions selected for evaluation ($u = \text{I, II, III, IV, V}$)
 j : indices for solutions that were evaluated with the models ($j = 1, \dots, n$)

Counters

- n : counter for the number model runs
 G_{fail} : counter for number of failures in improving upon best known solution

Functions

- $M(\cdot)$: objective function
 $\tilde{M}(\cdot)$: penalty-adjusted objective function
 $\tilde{c}_{max}(\cdot)$: $\max_r [C_r(\mathbf{P}^k, \tau^k)]$
 $s^M(\cdot)$: surrogate model for objective function
 $s^C(\cdot)$: Surrogate model for \tilde{c}_{max}
 $W(\cdot)$: weighted candidate score
 χ : function that indicates if a feasible solution was found
 μ : function that indicates if M_{max} was updated

Parameters

- n_0 : initial number of evaluated solutions
 n_{max} : maximum value for n
 $G_{max, fail}$: threshold for counter G_{fail}

Sets

- T : set for τ values
 P : set for \mathbf{P} values
 Λ : set for $M(\cdot)$ values
 Ψ : set for \tilde{c}_{max} values
 Ω : set for $\tilde{M}(\cdot)$ values (for SBSH-SP-P)

Algorithm Steps

1. Initialization:
 - 1.1. Set $n = n_0$ and $G_{fail} = 0$.
 - 1.2. Generate n initial candidates (\mathbf{P}_j, τ_j) .

- 1.3. Add vectors \mathbf{P}_j and τ_j to P and T, respectively, and initiate Λ , Ψ , and (for SBSH-SP-P) Ω as empty sets.
2. Evaluate initial candidates and select initial best solution:
 - 2.1. For each candidate (\mathbf{P}_j, τ_j) , compute $M(\mathbf{P}_j, \tau_j)$ and $\tilde{c}_{max}(\mathbf{P}_j, \tau_j)$, and add values to Λ and Ψ .
 - 2.2. If there are feasible solutions according to the $\tilde{c}_{max}(\mathbf{P}_j, \tau_j)$ values, the \mathbf{P}_j and τ_j vectors for the candidate with the lowest $M(\mathbf{P}_j, \tau_j)$ are labeled \mathbf{P}^{best} and τ^{best} , respectively, and the objective value is labeled M^{best} .
 - 2.2.1 For SBSH-SP-P: the highest feasible $M(\mathbf{P}_j, \tau_j)$ is labeled M_{max} , and $\chi = 1$. Otherwise, if there are no feasible solutions, M^{best} , \mathbf{P}^{best} and τ^{best} are assigned the values of the candidate with the lowest $\tilde{c}_{max}(\mathbf{P}_j, \tau_j)$, value, M_{max} is assigned a placeholder value, and $\chi = 0$.
For SBSH-SP-S: if there are no feasible solutions, M^{best} , \mathbf{P}^{best} and τ^{best} are assigned the values of the candidate with the lowest $\tilde{c}_{max}(\mathbf{P}_j, \tau_j)$.
 - 2.2.2 For SBSH-SP-P: For each initial point, compute $\tilde{M}(\mathbf{P}_j, \tau_j)$ and add values to Ω .
3. Fit surrogate model s .
 - 3.1 For SBSH-SP-P: Use information in P, T and Ω to fit surrogate model s^M .
For SBSH-SP-S: Use information in P, T and Λ to fit surrogate model s^M . Also, fit surrogate model s^C using information in P, T and Ψ .
4. Candidate point generation and selection:
 - 4.1. Generate candidates according to the rules of groups I through V.
 - 4.1.1 Eliminate candidates that do not pass the feasibility checks.
 - 4.1.2 For SBSH-SP-S: Eliminate candidates that are predicted to be infeasible according to s^C .
 - 4.2. For each group and each candidate k , compute $W(\mathbf{P}^k, \tau^k)$ using s^M .
 - 4.3. For each candidate group, select for model evaluation the candidate solutions with minimum $W(\mathbf{P}^k, \tau^k)$.
5. Candidate evaluation and updates of parameters and archives:
 - 5.1. Evaluate the five selected candidates u with the computationally expensive models to determine $M(\mathbf{P}^u, \tau^u)$ and $\tilde{c}_{max}(\mathbf{P}^u, \tau^u)$.
 - 5.2. If a feasible candidate $M(\mathbf{P}^{*u}, \tau^{*u})$ is better than M^{best} , or if there were no feasible solutions, set $M^{best} = M(\mathbf{P}^{*u}, \tau^{*u})$, $\mathbf{P}^{best} = \mathbf{P}^{*u}$, $\tau^{best} = \tau^{*u}$, and $G_{fail} = 0$. Otherwise, $G_{fail} := G_{fail} + 1$.
 - 5.2.1 For SBSH-SP-P: Update M_{max} if possible: If $\chi = 1$ and there is a feasible candidate u with $M(\mathbf{P}^u, \tau^u) > M_{max}$, then $M_{max} = M(\mathbf{P}^u, \tau^u)$. Else, if $\chi = 0$ and there are one or more of the five candidate points that are feasible, update M_{max} with the worst feasible $M(\mathbf{P}^u, \tau^u)$ and set $\chi = 1$. If M_{max} is updated, $\mu = 1$.
 - 5.2.2 For SBSH-SP-P: If $\mu = 1$, use the new M_{max} to update values in Ω , and then set $\mu = 0$.
 - 5.3 Increase counter $n := n + 5$, and add information from evaluated candidate points to Λ , Ψ , P, T, and Ω . If $n \leq n_{max}$ return to step 3; otherwise, continue to step 6
6. Return \mathbf{P}^{best} and τ^{best}

3.3.4 SBSH for Multi-Objective Area Pricing Design Problems

In addition to the pollutant concentration constraints, Problem 2 considers two objectives that are not necessarily complementary: improving travel conditions and reducing the environmental impact of traffic. The available single-objective optimization heuristics cannot be applied to solve this problem, nor do they consider constraints beyond the closed boundary requirement, so in this section a new SBSH for constrained multi-objective ACP problems (SBSH-MP) is proposed. The algorithm consists of the following general steps. In each iteration a set of good solutions are selected from an archive of previously evaluated solutions, and based on these solutions a pool of candidates is generated. From this candidate pool, the solutions that

are predicted to be feasible and to dominate all other solutions (according to the surrogate models) are selected. From these a single solution is picked according to one of three selection rules. This promising solution is evaluated via the computationally expensive models, and the process repeats itself until a maximum number of iterations is reached. In this subsection, the procedures to generate the candidate solutions and to select the most promising candidate are presented, as well as the steps of SBSH-MP.

3.3.4.1 Procedures to Generate Candidate Solutions in SBSH-MP

One of three types of candidate solutions are generated in each iteration of SBSH-MP. Which type of candidate solution is generated in an iteration is randomly determined. Type I, Type II, or Type III solutions are generated with probabilities Γ^I , Γ^{II} , and Γ^{III} , respectively, in each iteration. If Type I solutions are selected, then N^I polygons are randomly generated. Each group I polygon is replicated $|\tau|$ times, and the replicated polygons are assigned a different toll level from the τ set. Type II and type III solutions are generated based on the information of the best known solutions at a particular iteration. The best solutions are those that satisfy the concentration constraint and are non-dominated. In the context of this study, a solution dominates another solution if it has a lower M objective value and its H objective value is no worse than the competitor's value, or if it has a lower H objective function value and its M value is no worse than the competitor's value. Non-dominated solutions are identified using a Pareto ranking procedure (Deb et al., 2002).

In the case of type II solutions, a number $b^{seed,II}$ of seed solutions are selected from the set of non-dominated solutions Λ^{nd} . If the number of solutions in the non-dominated set ($|\Lambda^{nd}|$) is less than $b^{seed,II}$, then the available non-dominated solutions are replicated until there are $b^{seed,II}$ seeds. On the other hand, if $|\Lambda^{nd}|$ is greater than $b^{seed,II}$, then the crowding distance of each of the best known solutions is computed, and the $b^{seed,II}$ solutions with the highest crowding distance are selected. The crowding distance metric measures a solution's proximity to other solutions in the objective function space; the greater the crowding distance, the farther away is a solution from other solutions. That is, crowding distance is an indicator of the level of uniqueness of a solution. In the numerical example, a solution's crowding distance was defined as the product of the Euclidean distances to its two closest neighbors (in the objective function space). The last possible scenario is that there are no feasible solutions, in which case the $b^{seed,II}$ solutions that violate the least the concentration constraint are selected. After the $b^{seed,II}$ solutions are identified, the polygon associated with each seed is replicated $|\tau|$ times, and, as before, the replicated polygons are assigned a different toll level from the τ set, except for the toll already considered in the corresponding $b^{seed,II}$ solutions. The type II solutions have the same charging boundary as the seed solutions, but they have different toll values.

Type III solutions are generated using $b^{seed,III}$ seed solutions that are selected using the same strategies as the ones discussed for type II solutions, but in this case the charging boundaries are modified. Similar to SBSH-SP, in SBSH-MP there are three boundary modification operations: expansion, contraction, and both expansion and contraction. For each type of operation there are two modes: uncoordinated and coordinated. These operations follow the same procedures as the ones for the type III candidate group in SBSH-SP, with the difference that, instead of anchoring the perturbations in a solution \mathbf{P}^{best} , here the solutions are generated based on the information of the non-dominated seed solutions.

3.3.4.2 Candidate Selection Procedure

The selection of the most promising candidate solution follows three steps: (i) the identification of candidates that are predicted to be feasible, (ii) the identification of non-dominated candidates, and (iii) the selection of a solution that satisfies a performance criterion. In each iteration, the surrogate models guide the selection of the candidate solution that is then evaluated by the computationally expensive models. Let \mathbf{X}^0 represent the set of all previously evaluated candidate designs, and Ω^M , Ω^H , and

Ψ represent the corresponding M and H objective values and the constraint value, respectively. First, the information stored in \mathbf{X}^0 and Ψ is used to fit a surrogate model s^C . s^C is then utilized to predict the value of the concentration constraint for each candidate solution k . For each k , if the surrogate model predicts that the concentration constraint is violated (i.e., $s^C(\mathbf{P}^k, \tau^k) > C_{max}$), the solution is discarded; otherwise, the solution is preserved. Next, surrogate models for the objective functions M and H are fitted with the data in sets \mathbf{X}^0 , Ω^M , and Ω^H . Based on the predicted objective function values, the candidate solutions that are expected to be non-dominated are selected. For notational simplicity, let $\boldsymbol{\mu}^k = \{\mathbf{P}^k, \tau^k\}$ be a candidate solution predicted to be non-dominated (with $\boldsymbol{\mu}^k \in \mathbf{X}$) on the basis of its predicted mobility objective function value $\hat{M}(\boldsymbol{\lambda}^k)$ and its environmental inequality objective function value $\hat{H}(\boldsymbol{\lambda}^k)$.

In the final stage of the selection process a single solution $\boldsymbol{\mu}^*$ is selected based on one of the following three rules. The first rule selects the $\boldsymbol{\mu}^k$ with the maximum minimum domain distance relative to all previously evaluated solutions. That is,

$$\mathbf{X}^* = \arg \max_{\boldsymbol{\mu}^k \in \mathbf{X}} \left(\min_{\boldsymbol{\mu}^0 \in \mathbf{X}^0} \|\boldsymbol{\mu}^k - \boldsymbol{\mu}^0\| \right) \quad (20)$$

The $\boldsymbol{\mu}^*$ under the second rule is the $\boldsymbol{\mu}^k$ with the maximum minimum objective space distance relative to previously evaluated solutions, defined here as:

$$\boldsymbol{\mu}^* = \arg \max_{\boldsymbol{\mu}^k \in \mathbf{X}} \left(\min_{\boldsymbol{\mu}^0 \in \mathbf{X}^0} \sqrt{[\hat{M}(\boldsymbol{\mu}^k) - M(\boldsymbol{\mu}^0)]^2 + [\hat{H}(\boldsymbol{\mu}^k) - H(\boldsymbol{\mu}^0)]^2} \right) \quad (21)$$

Under the third rule, the $\boldsymbol{\mu}^k$ that results in the maximum predicted improvement in the dominated objective space is selected. Let $A(\mathbf{X}^0)$ be the area of the objective space that is dominated by the solutions in \mathbf{X}^0 . Then the maximum predicted improvement in dominated space is defined as:

$$\boldsymbol{\mu}^* = \arg \max_{\boldsymbol{\mu}^k \in \mathbf{X}} [A(\mathbf{X}^0 \cup \boldsymbol{\mu}^k) - A(\mathbf{X}^0)] \quad (22)$$

If no solution is predicted to adjust the dominated space, then the algorithm selects a solution according to the first rule. The selected $\boldsymbol{\mu}^*$ candidate is then evaluated by the computationally expensive models. The algorithm cycles, in order, through a different rule in each iteration. The three-rule strategy used in this last stage of the selection process was adapted from the work of Akhtar and Shoemaker (2016).

3.3.4.3 Steps of SBSH-MP

Next, the SBSH-MP steps, and associated notation, are presented.

Decision variables

- τ : charging area toll level
- \mathbf{P} : vertices defining changing area boundary

Counter and Index

- n : counter for the number of solutions evaluated with the computationally expensive models, and identifier for the evaluated solutions

Functions

- s^M : surrogate model for the M objective
- s^H : surrogate model for the H objective
- s^C : surrogate model for the pollutant concentration function

Parameters

- n_0 : initial number of evaluated solutions
- n^{max} : maximum value for n

Sets

- \mathbf{X}^0 : set of evaluated solutions
- Ω^M : Set containing the M objective function value for evaluated solutions
- Ω^H : Set containing the H objective function value for evaluated solutions
- Ψ : Set containing the constraint function value for evaluated solutions

Algorithm Steps

1. Initialization:
 - 1.1. Set $n = n_0$.
 - 1.2. Generate n initial candidates (\mathbf{P}^n, τ^n) .
 - 1.3. Add points (\mathbf{P}^n, τ^n) to \mathbf{X}^0 and initiate Ω^M , Ω^H , and Ψ as empty sets.
 - 1.4. Evaluate initial candidates with the computationally expensive models and store the results in sets Ω^M , Ω^H , and Ψ .
2. Generate type I, type II, or type III candidate solutions, and select those candidates that meet the shape constraints and that have not been previously evaluated.
3. With the information in sets \mathbf{X}^0 , Ω^M , Ω^H , and Ψ fit the surrogate models s^M , s^H , and s^C for the mobility and environmentally-oriented objective functions and the pollutant concentration function.
4. Using s^M , s^H , and s^C , predict the objective function values and concentration function value for each candidate.
5. Select μ^* according to the candidate selection procedure:
 - 5.1. Select the candidates that are predicted to satisfy the concentration constraint according to s^C .
 - 5.2. Select the candidates that are expected to be non-dominated according to s^M and s^H .
 - 5.3. From the surviving solutions, select μ^* according to the three-rule strategy.
6. Evaluate μ^* with the computationally expensive models, and store μ^* and the model outputs in \mathbf{X}^0 , Ω^M , Ω^H , and Ψ .
7. If $n > n^{max}$, return the set of non-dominated solutions in \mathbf{X}^0 , Ω^M , Ω^H , and Ψ . Otherwise, set $n = n + 1$ and return to step 2.

4 Tests and Results

An illustrative application of the proposed models and solution heuristics is presented in this section. The SBSH-SP is applied with three different objectives:

- Maximization of consumer surplus function, M^{CS}
- Minimization of deviations from status quo deviation, M^{SQ}
- Minimization of collected revenue, M^{Rev}

The two objectives considered in the application of the SBSH-MP are:

- Maximization of consumer surplus function, M^{CS}
- Minimization of environmental inequality (i.e., Atkinson index), H^A

The accuracy of surrogate models in the context of this type of design problem is also explored. All tests were performed using the Chicago Sketch Network.

4.1 Test Problems Setup

Only the road network within the Cook and DuPage counties was employed, which, in the Chicago Sketch Network, is composed of 1,330 links and 421 nodes, including 160 origin-destination zones (see Figure 5). Base information of the demand and trip distribution in the test network was obtained from an online repository (Bar-Gera, 2014). The base demand data was augmented to create four time-of-day travel demand periods. The toll set τ contained tolls ranging from \$1 to \$20, with \$1 increments. Homogeneous network users with a value of time of \$30 per hour were assumed.

Simple polygons with 12 vertices defined the charging boundary. The reference point O was located in Chicago's central business district (coordinate (710070, 1931400) in node system (Bar-Gera, 2014)). Radii could assume values in the interval [16500, 75500] (feet). The angles were bounded to [1.8, 5] (radians), with two vertices fixed at angles 1.8 and 5 radians.

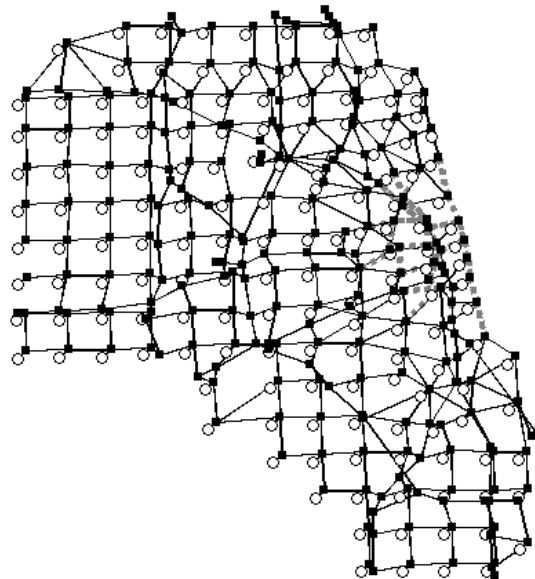


Figure 5. Abridged Chicago Sketch Network

4.1.1 Models

The inputs necessary to compute objectives and constraint for the design problems were generated via a four-component model system. First, network flows were computed using a standard, sequential planning model composed of a trip distribution model, a mode split model, and a traffic assignment model. Part of the demand was assumed to have a fixed distribution, while another portion was distributed using a logit destination choice model. A destination's attractiveness was specified as a function of its level of employment and the corresponding mode choice logsum variable. The mode split model was formulated as a binary logit model with only auto and transit as travel alternatives. A deterministic user equilibrium (DUE) model was used to assign traffic flows on the road network. The DUE problem was solved via the gradient projection method (Jayakrishnan et al., 1994). For simplicity, a multinomial logit model was used to assign transit flows. The three shortest paths were identified for each origin-destination pair, and transit flows were assigned to these paths based on travel time, cost, and average load factor (ratio of the demand on a link and its capacity) throughout the length of the path. The method of successive averages was utilized as the feedback procedure (Boyce et al., 2008). Based on the outputs of these models the M objectives were computed. For the consumer surplus objective M^{CS} the marginal utility of income was set to one (extending the idea of a homogeneous population). Also, the logsums of the base scenario were dropped from the objective function, as these are constants.

Link emissions were computed using an average-speed emission model that is a function of the link flows and average speeds computed in the travel demand model. Nitrogen dioxide (NO_2) was selected as the pollutant of interest. Speed-based emission factors for NO_2 were obtained from EPA's MOVES model (EPA, 2014). Given the link emissions, a simple street canyon model was used to compute concentrations at receptor points (Venegas et al., 2014). Two receptors per street canyon (one per canyon face) were assumed. A different meteorological scenario (with distinct wind speeds and directions) was specified per time-of-day period. The C_{max} for the NO_2 concentrations was set to be five percent lower than the maximum concentration observed in the base, no-toll condition.

For problem 2, the agent-level intake measures were computed after the link travel times, origin-destination travel paths, and pollutant concentrations were modeled. The initial itinerary of the individuals was generated based on the household travel survey data collected from Chicago Metropolitan. The dataset includes the information on the set of activities conducted by travelers on a given day along with the information on the activity duration, location, schedule and the mode used to perform the activity. To compute the intake, agents were given the same breathing rate of 12.2 cubic meters per day. Having computed the agent's NO_2 intake, the Atkinson index was determined with a 0.75 inequality aversion parameter.

The previous model system takes a relatively short amount of time to evaluate (about 8 minutes in using 12 cores of Precision T7910 with 144 GB of RAM). Naturally, the more detailed models used in practice could take up to a day to run.

4.1.2 Algorithm Parameters

Ten trial runs per problem specifications were performed for the single objective design problems, and five trial runs were performed for the bi-objective design problem. A trial run was initialized with 100 solutions, and an additional 150 candidate designs were evaluated in each run (i.e., n^{max} was set to 250 for the trial runs of SBSH-SP and SBSH-MP). The averaged results from these trial runs are reported in section 4.1.4. The parameter values for the SBSH-SP and SBSH-MP trials are reported in Table 1 and Table 2, respectively. The convexity index was set to 0.45 (Maruyama et al., 2014), and ϱ was defined as 0.8 radians.

Table 1. Parameter Values used in the SBSH-MP Trial Runs

Parameter	Value
ε	5
D^{II}	10
D^{III}	4000
D^{IV}	1000
Γ^U	0.60
Γ^{mut}	0.02
$[\omega^{min}, \omega^{max}]$	[0,0.1]
$[\omega^{\delta,min}, \omega^{\delta,max}]$	[0.8,1]
d^{max}	0.40
σ^2	0.05
$G_{max,fail}$	20
κ	1000
Υ	[0.95,0.97,1]
Υ^{GA}	[0.70,0.85,0.90,0.95,1]

Table 2. Parameter Values used in the SBSH-MP Trial Runs

Parameter	Value
Γ^I	0.05
Γ^{II}	0.20
Γ^{III}	0.75
Γ^U	0.60
$b^{seed,II}$	5
$b^{seed,III}$	5
$[\omega^{min}, \omega^{max}]$	[0,0.1]
$[\omega^{\delta,min}, \omega^{\delta,max}]$	[0.8,1]
d^{max}	0.40
σ^2	0.05

4.2 Results for the Surrogate Models' Accuracy and Correlation Tests

A geometric representation of a charging area's boundary is arguably intuitively reasonable. However, it is an open question whether this data representation is useful within a surrogate optimization-based framework as inputs to the model approximations. For this reason, a series of tests were conducted to explore the predictive accuracy of surrogate models estimated using the proposed simple polygon representation of charging boundaries, as well as the correlation of the predictions relative to the actual model outputs. Two sets of tests were conducted using a sample of 500 charging schemes created by randomly generating charging boundaries (polygons) and associated tolls. In the first set of tests the difference between the surrogate predictions and the actual model values was examined. The second set of tests examined the utility of the surrogate predictions in the classification of solutions as either feasible or infeasible on the basis of the pollutant concentration threshold. The predicted class membership (i.e., feasible or infeasible) was compared with the actual class membership, as indicated by each solution's modeled maximum concentration.

Four types of surrogate models were tested: radial basis functions with linear form (i.e., linear RBF), cubic RBF, thin plate spline RBF (Gutmann, 2001), and a second-degree polynomial model (Khuri and Mukhopadhyay, 2010). In the first set of tests a series of k-fold cross validation tests were performed for each surrogate model type. In k-fold cross validation the sample is divided into K partitions. A partition k is used once as the validation data set, while the remaining partitions are used to fit the surrogate model; this is repeated for all partitions. Folds of 2, 5, and 10 were used in the tests, with sampling for each fold performed 30 times. In addition to the k-fold cross validation tests, cross validation tests were performed by randomly selecting 100 data points (candidate schemes) as the training data set, while the remaining 400 data points were used for validation. Again, these tests were repeated 30 times.

In the first set of tests, the surrogate's predictive accuracy and correlation with the actual model outputs was quantified using models for the: consumer surplus objective (M^{CS}), the status quo objective (M^{SQ}), the revenue objective (M^{Rev}), consumer surplus objective adjusted by the penalty method (equation 16, Penalty M^{CS}), and the maximum concentration constraint (\tilde{c}_{max}). Table 3 reports the correlation between the surrogate predictions and the real function values (Pearson correlation coefficient; PC), as well as the mean average percent error (ME). The best results in each test category are in bold (e.g., a 0.69 correlation of the linear RBF surrogate was the highest for 100/400 cross-validation test for Penalty M^{CS}). On average, the worst results were obtained for the second-degree polynomial models. The RBF surrogates obtained similar results, although, the results suggest that the best surrogate model is the thin-plate spline RBF. The thin-plate spline surrogate obtained its lowest ME for the \tilde{c}_{max} function (lower than 1 percent). Another noteworthy result are the large mean errors (over 150%) and moderately good correlation (over 0.70 for RBFs) in the Penalty M^{CS} tests, which are significantly worse than the results obtained for the other functions. This result is to be expected as the penalty method dramatically adjusts the objective function value as a function of constraint violations, which has the effect of creating a discontinuous objective function space.

Table 3. Results for Cross-Validation Tests

Type	TEST	M^{CS}		M^{SQ}		M^{Rev}		Penalty M^{CS}		\tilde{c}_{max}	
		CP	ME	CP	ME	CP	ME	CP	ME	CP	ME
Cubic RBF	K = 2	0.998	2.64	0.996	22.63	0.985	7.32	0.716	203.85	0.987	1.07
	K = 5	0.998	4.19	0.997	14.54	0.982	6.47	0.771	116.54	0.987	0.99
	K = 10	0.998	3.58	0.998	15.37	0.985	6.20	0.805	121.07	0.989	0.86
	100/400	0.998	3.96	0.994	25.49	0.978	9.29	0.633	154.44	0.970	1.59
Thin-Plate RBF	K = 2	0.998	1.96	0.997	19.26	0.987	6.80	0.718	189.21	0.989	0.95
	K = 5	0.999	3.09	0.998	14.28	0.985	5.78	0.778	109.35	0.990	0.90
	K = 10	0.998	2.87	0.998	13.75	0.987	5.77	0.811	113.55	0.990	0.78
	100/400	0.998	3.87	0.994	22.10	0.980	8.84	0.643	143.20	0.971	1.53
Linear RBF	K = 2	0.998	1.24	0.996	14.14	0.986	9.22	0.717	169.12	0.986	1.14
	K = 5	0.998	3.23	0.997	12.20	0.985	6.54	0.784	97.59	0.987	0.99
	K = 10	0.998	3.29	0.997	12.30	0.987	6.62	0.809	108.79	0.989	0.87
	100/400	0.995	3.35	0.992	20.09	0.980	11.47	0.690	122.07	0.963	1.76
Polynomial	K = 2	0.986	7.97	0.956	70.57	0.881	26.84	0.345	326.74	0.834	4.37
	K = 5	0.992	9.11	0.974	39.31	0.927	17.41	0.398	206.24	0.890	3.05
	K = 10	0.995	6.22	0.981	34.66	0.951	13.46	0.415	202.18	0.914	2.62
	100/400	0.995	6.29	0.977	44.85	0.945	16.85	0.408	221.01	0.904	2.87

Figure 6 reports the results obtained for the solution classification tests. The thin-plate RBF model was used. In four classification test runs the C_{max} threshold was set to be lower than the base maximum pollutant concentration by 5, 15, 20, and 25 percent, respectively. The figure consists of so called confusion matrices that report the proportions of correct classification given the surrogate predictions and the modeled (actual) classification (e.g., true negative: solution was predicted to be infeasible and it is actually infeasible according to the \tilde{c}_{max} result) and the proportions of incorrect classifications (e.g., false negative: solution was predicted to be infeasible and it is actually feasible). The results of the trial runs show a high degree of classification accuracy, with the highest misclassification at 7 percent for the C_{max} set to be 20 percent lower than the base maximum concentration. These results are not too surprising given the low ME obtained for the \tilde{c}_{max} function, but they should not be generally expected since it is unlikely that the output of \tilde{c}_{max} -type functions will usually be easy to accurately predict.

Overall, the cross-validation tests for the surrogate models provide evidence for the potential usefulness of the geometric representation of charging boundaries in surrogate-based solution heuristics, as well as showing, once again, that available surrogate models provide relatively good approximations to commonly used models in transportation engineering planning. In the application tests of the SBSHs, the thin plate spline RBF was used, given the results for the test problems considered here.

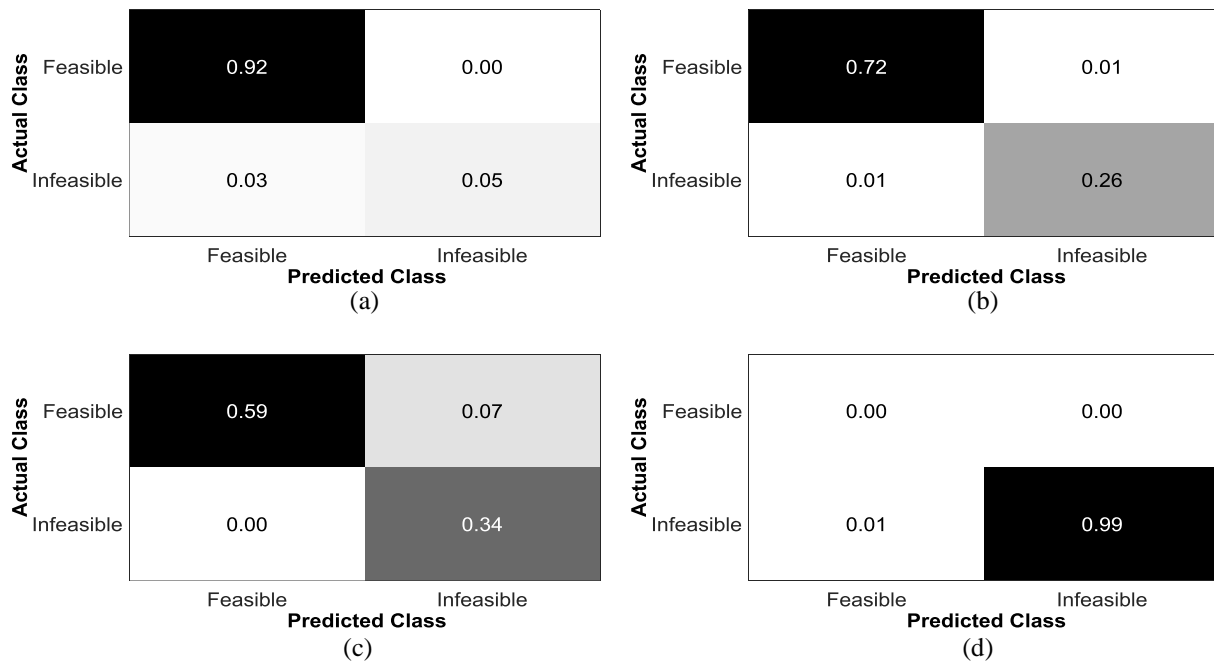


Figure 6. Confusion matrix for solution feasibility tests

4.3 Results for Single-Objective Design Problem

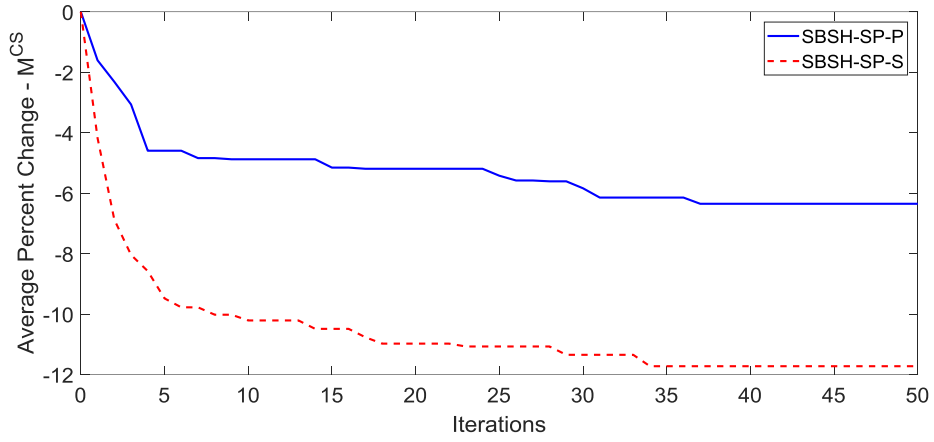
As mentioned in the introduction of this section, the SBSH-SP was tested for three constrained, single-objective problems for the design of area pricing schemes. Figure 7 shows the average percent change relative to each run's best initial design for the single objective problem with the M^{CS} , M^{SQ} , and M^{Rev} objectives, respectively. On average, the best solutions generated by the SBSH-SP for the M^{CS} , M^{SQ} , and M^{Rev} problems had objective function values that were approximately 12%, 11%, and 8% lower than the best solution in the initial pool of solutions. In terms of which version of the SBSH-SP heuristic is best, the results are mixed: the penalty-based method (SBSH-SP-P) was markedly outperformed by SBSH-SP-S in the M^{CS} problem, but it resulted in the best results in the other two problems. In the initial iterations of the trial runs, however, the SBSH-SP-S found, on average, better results in the M^{SQ} and M^{Rev} problems.

This is significant as there can be design problems in which 250 (100 initial solutions plus 150 extra evaluations) design evaluations would take too much time relative to the time available for analysis. So, for instance, SBSH-SP-S would be the best performing heuristic in all the problems considered here if there was time for only 10 iterations of the solution heuristic.

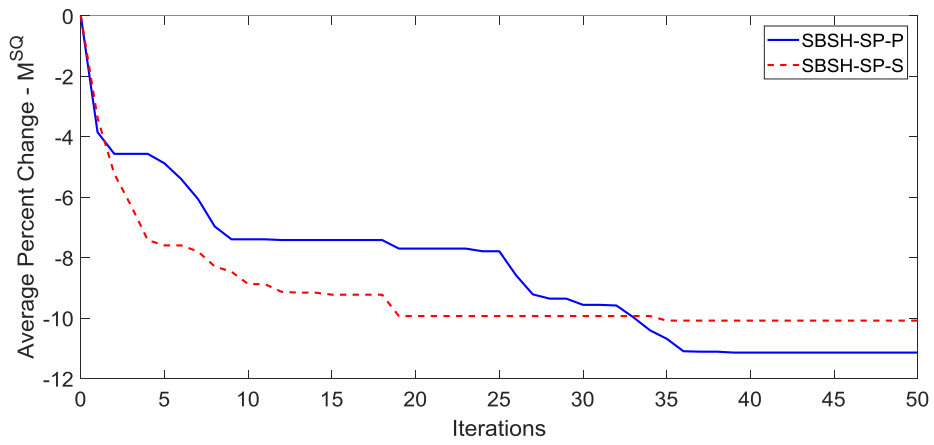
For each problem considered, Figure 8 shows how the diversity in the pool of evaluated solutions evolves as more candidate solutions selected by the SBSH-SPs are evaluated (i.e., as more solutions are added to the pool of evaluated solutions). Diversity here refers to the variability that exists between solutions. In the language of evolutionary algorithms, the genotypic diversity is of interest in this analysis, that is, diversity in terms of the differences between the sets of decision variables that define different designs. The moment of inertia measure proposed by Morisson and de Jong (2001) is used to quantify diversity. The moment of inertia (normalized by the population size and the initial inertia level in each trial) was computed for the geometric representation of the charging scheme ((\mathbf{P}, τ) diversity) and for their corresponding η representation ($(\boldsymbol{\eta}, \tau)$ diversity). As expected, as the heuristics explore the most promising solution space, the degree of diversity generally reduces. As the units of the (\mathbf{P}, τ) and $(\boldsymbol{\eta}, \tau)$ representations are different, no meaningful comparison can be made regarding differences between these two curves. However, both curves show that SBSH-SP-S maintains more diversity in its pool of solutions, which is positive since it is less likely to be trapped on a local minimum, but negative because it might mean that the search jumps away to areas of the solution space that, although they may add diversity, are unlikely to result in a better design. The latter is an important consideration since in the application context of interest there are only relatively few solutions that can be evaluated.

Figure 9 presents examples of the all the polygons generated in three trial runs of SBSH-SP-S for the three planning problems considered, along with the toll level associated with the best charging boundary. In each figure in Figure 9, the 150 polygons generated during the trial run are plotted (blue lines), along with the best simple polygon (red line) and the maximum extension of the charging area (black polygon) (the boundaries for the 100 initial solutions are not plotted). As it can be seen in the figure, there is a concentration of polygons around the best solution, which is to be expected given that three of the five strategies that compose the candidate generation procedure search for solutions based on the information of the best known solution at the time.

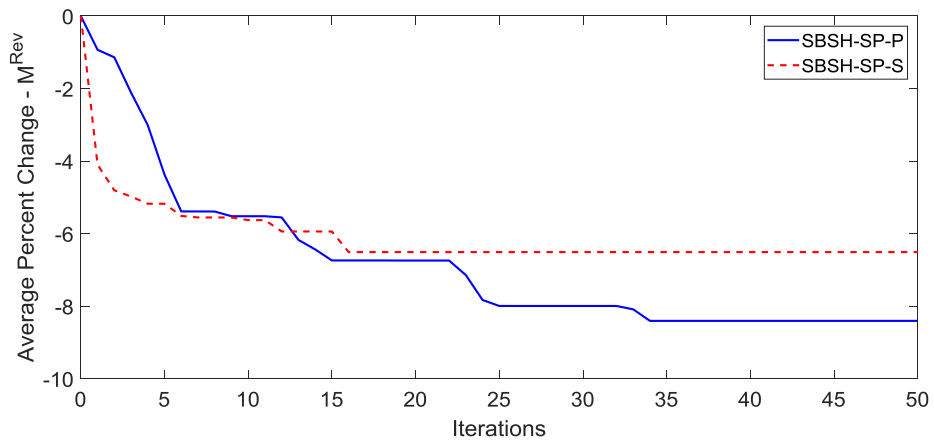
Obviously, the observations made in these tests are specific to the particular problems considered; different problems with different networks and model systems could suggest the opposite of what has been shown here regarding the performance of SHBS-SP-P vis-à-vis SHSB-SP-S. Nevertheless, the tests show that the proposed heuristics and, particularly, the geometric-based representation of charging boundaries and the surrogate model predictions that constitute the heuristics, can be used to search for solutions to ACP design problems with a single planning objective.



(a)

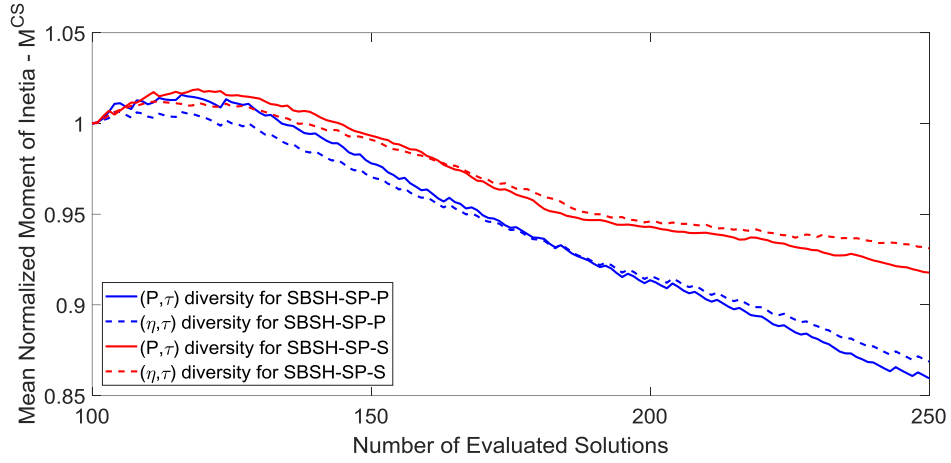


(b)

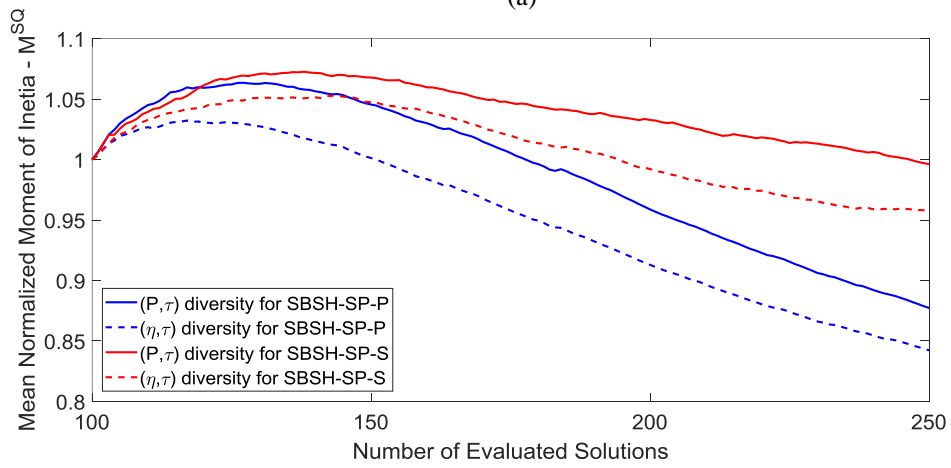


(c)

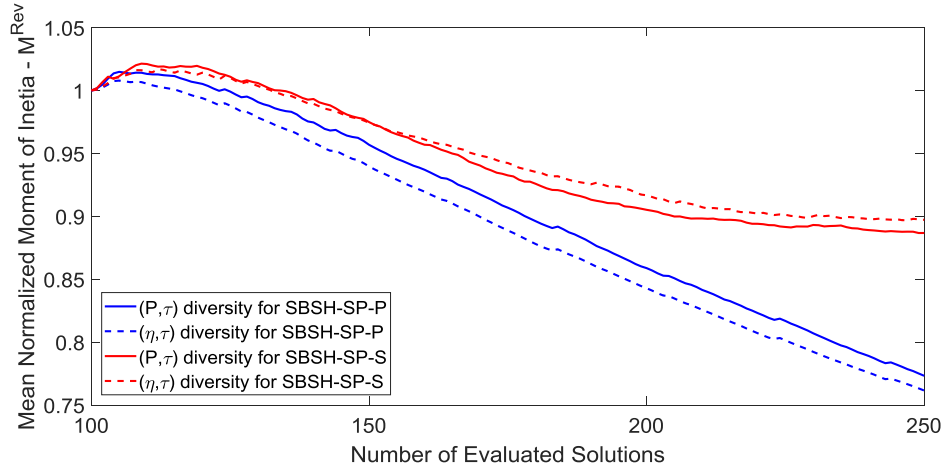
Figure 7. Progression in average percent improvement relative to best initial designs for single-objective problems



(a)



(b)



(c)

Figure 8. Progression of the average diversity levels of the solution pool for the SBSH-SPs

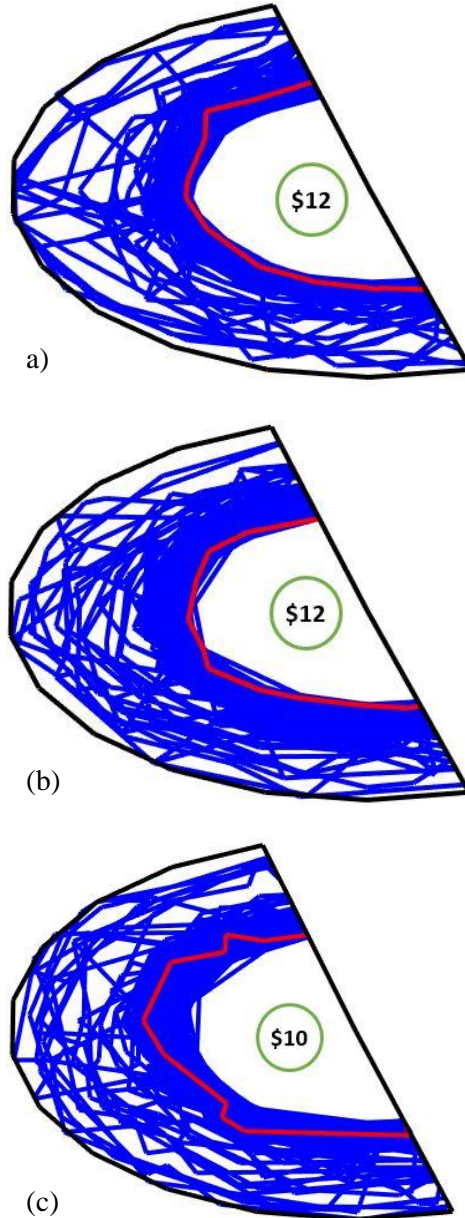


Figure 9. Example of generated polygons in trial runs with the a) M^{CS} , b) M^{SQ} , and c) M^{Rev} objectives

4.4 Results for Bi-Objective Design Problem

Figure 10 shows that in each iteration of the SBSH-MP there is a steady improvement in the objective space dominated by the evaluated solutions. This figure shows the average improvement in dominated objective function space relative to the objective function space dominated by the initial pool of solutions. By the 150th candidate evaluation, the final pool of solutions dominated, on average, 49.3 percent more objective space than the initial pool of solutions. The results suggest that the proposed heuristic is capable of identifying relatively good solutions in the context a bi-objective problem in which the number of function evaluations is significantly constrained.

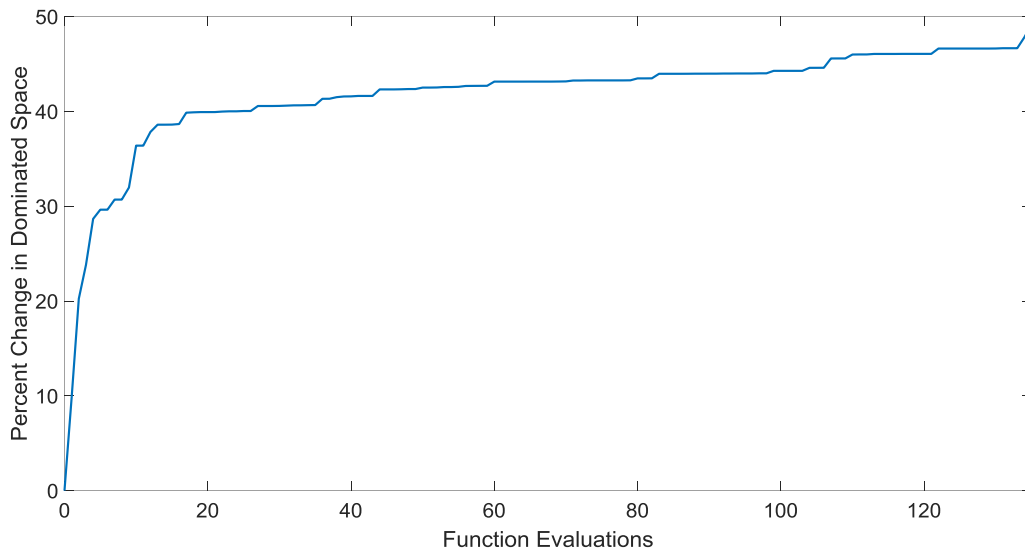


Figure 10. Average improvement in dominated objective space

As an example, in Figure 11, the normalized objective function values for the initial solutions and the solutions generated by the SBSH-MP in a trial run are presented. Most of the solutions selected by the algorithm are feasible (97 percent).

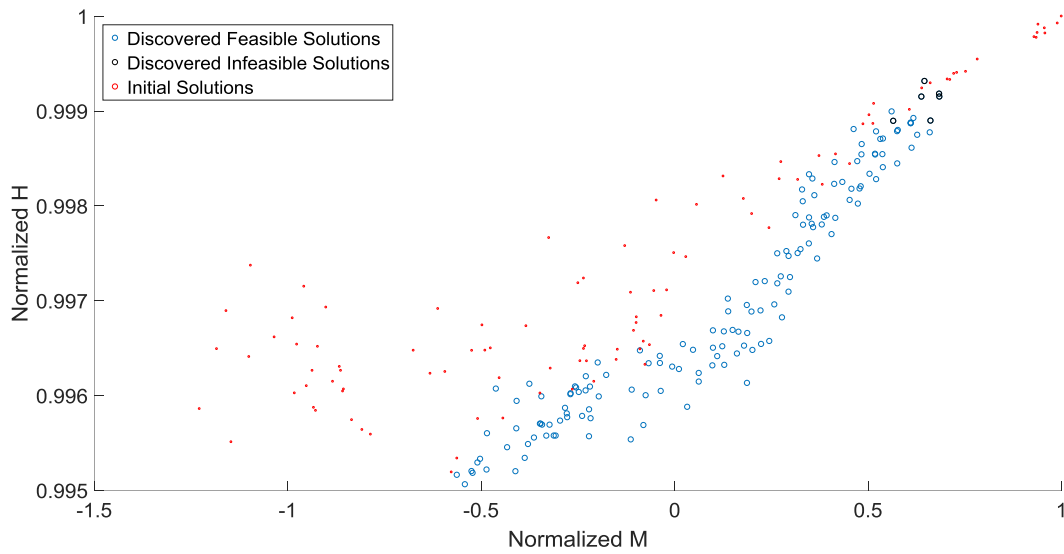


Figure 11. Example of the distribution of a pool of solutions' objective values for a trial run

5 Summary and Potential Research Opportunities

The main research contributions of this project are as follows:

- *Environmentally-oriented optimization problems for the design of ACP schemes:* In addition to the single objective planning problem with environmental constraints, an ACP design problem was presented that incorporates activity-based measures of agents' exposure to vehicle-generated air pollutants, a metric that is used to account for the often-ignored goal of reducing environmental inequality in transportation planning interventions.
- *Surrogate-based solution heuristics for single- and multi-objective ACP design problems:* Two heuristics were proposed to solve optimization problems for ACP design. The heuristics utilize a geometric representation of charging boundaries, which is used to fit surrogate models that are then used in the search of good problem solutions. The results of the numerical tests generally showed a strong correlation between the surrogate model predictions and the outputs of different models, thus suggesting that the geometric representation of charging boundaries, coupled with surrogate models, can be useful elements of solution heuristics. Tests with the proposed heuristics also suggest that the algorithms can find solutions that are substantial better than the initial solution pool.
- *A new network-based, activity model for travel demand analysis:* An activity-based model was developed to infer the mobility behavior of travelers in response to change in the network and cost of travel. The Household Activity Pattern Problem was utilized as the core behavioral model, which was extended to incorporate variable travel time and mode choice (for two modes of transportation, bus and car).

The ultimate goal of this research project was to create a practical methodology for the optimization-based design of ACP schemes. To this end, future research could focus on the development of modeling frameworks that would reduce the computational burden of employing, within the context of an optimization model, an agent-based simulation of the travel and activity patterns of all agents in the study region. For example, a procedure could be developed in which the aggregate outputs of agent-based behavioral models are approximated using metamodels that are conceptually similar to incremental demand models (or pivot models). Assuming that only aggregate outputs are of interest, the metamodels could offer a relatively quick way of modeling the impacts of changes in features of the transportation system. If the metamodels are shown to be good approximations, this strategy could change the way agent-based models are employed in practice. Another practical consideration is the formulation of ACP design problem that consider how the revenue generated by the road pricing scheme is reinvested in the transportation network. An example of this type of model is a planning problem that jointly considers the design of transit networks and ACP schemes.

Research extensions could also focus on the geometry-based representation of charging boundaries. In this project, boundaries were represented using simple polygons. However, there is a vast literature on shape optimization that could be relevant to ACP problems. It is possible that alternative models for boundary shape representation could offer a richer and more useful encapsulation of the information that defines a charging boundary.

Lastly, the HAPP model can be extended to predict the elasticity of mobility patterns with respect to changes in different policies, which might directly or indirectly impact the overall utility gained by the travelers by moving in the networks and conducting their daily activity routines.

References

- Adler, T., Ben-Akiva, M., 1997. A theoretical and empirical model of trip chaining behavior. *Transportation Research Part B*,13(3): 243-257.
- Akhtar, T., Shoemaker, C.A., 2016. Multi objective optimization of computationally expensive multi-modal functions with RBF surrogates and multi-rule selection. *Journal of Global Optimization*, 64: 17-32.
- Allahviranloo, M., R. Regue, Recker, W.W., 2014. Pattern clustering and activity inference. Presented at the 93rd Annual Meeting of the Transportation Research Board, Washington, D.C.
- Allahviranloo, M., Recker, W.W., 2013. Modeling uncertainty in households' activity engagement decisions. Presented at the 92nd Annual Meeting of the Transportation Research Board, Washington, D.C.
- Arentze, T., F. Hofman, H. van Mourik, Timmermans, H., 2000. ALBATROSS: multiagent, rule-based model of Activity pattern decisions. *Transportation Research Record*, 1706: 136-144.
- Auld, J., Mohammadian, A.K., 2012. Activity planning processes in the agent-based dynamic activity planning and travel scheduling (ADAPTS) model. *Transportation Research Part A*, 46(8): 1386-1403.
- Bhat, C. R., J. Y. Guo, S. Srinivasan, Sivakuma, A., 2004. A comprehensive econometric micro-simulator for daily activity-travel patterns (CEMDAP). *Transportation Research Record*, 1894: 57-66.
- Boyce, D., O'Neill, C.R., Scherr, W., 2008. Solving the sequential travel forecasting procedure with feedback. *Transportation Research Record*, 2077: 129-135.
- Brownstone, D., Small, K.A., 1989. Efficient estimation of nested logit models. *Journal of Business & Economic Statistics*, 7(1):67-74.
- Caiazza, F., Ashok, A., Waitz, I.A., Yim, S.H.L., Barrett, S.R.H., 2013. Air pollution and early deaths in the United States. Part I: Quantifying the impact of major sectors in 2005. *Atmospheric Environment*, 79: 198-208
- Castiglione, J., Bradley, M., Glied, J., 2015. Activity-based travel demand models. SHRP 2 Report S2-C46-RR-1.
- Chen, X., Zhang, L., He, X., Xiong, C., 2014. Surrogate-based optimization of expensive-to-evaluate objective for optimal highway toll charges in transportation network. *Computer-Aided Civil and Infrastructure Engineering*, 29: 359-381.
- Chen, X., Zhu, Z., He, X., Zhang, L., 2015. Surrogate-based optimization for solving a mixed integer network design problem. *Transportation Research Record*, 2497: 124-134.
- Chow, J.Y.J. and Regan, A.C., 2014. A surrogate-based multiobjective metaheuristic and network degradation simulation model for robust toll pricing. *Optimization and Engineering*, 15(1): 137-165.
- Chow, J.Y.J., Recker, W.W., 2012. Inverse optimization with endogenous arrival time constraints to calibrate the household activity pattern problem. *Transportation Research Part B*, 46(3): 463-479.

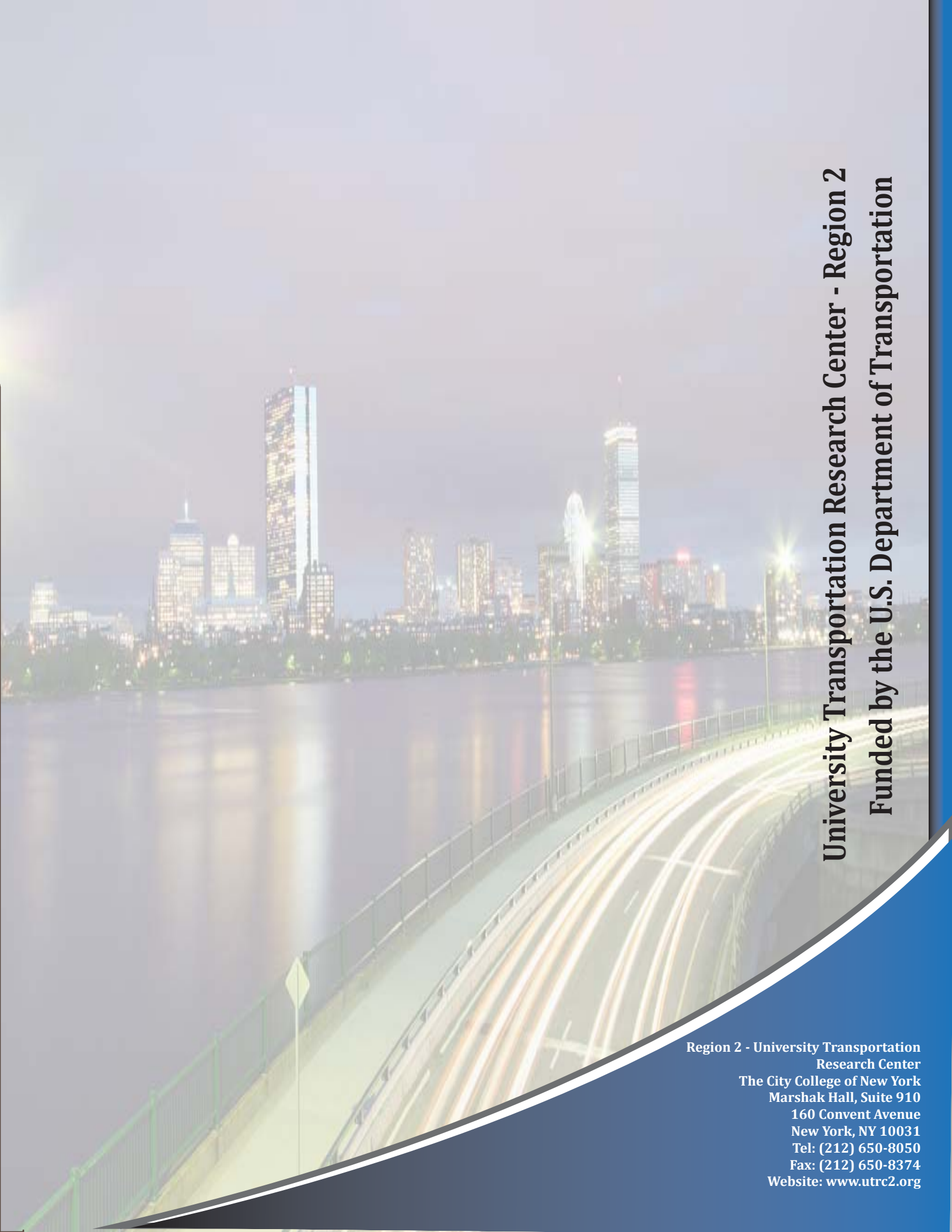
- Chow, J.Y.J., Regan, A.C., Arkhipov, D.I., 2010. Faster converging global heuristic for continuous network design using radial basis functions. *Transportation Research Record*, 2196: 102-110.
- de Jong, G., Daly, A., Pieters, M., van der Hoorn, T., 2007. The logsum as an evaluation measure: Review of the literature and new results. *Transportation Research Part A*, 41: 874-889
- Deb, K., 2000. An efficient constraint handling method for genetic algorithms. *Computer Methods in Applied Mechanics and Engineering*, 186:311-338.
- Deb, K., A. Pratap, S. Agarwal, and Meyarivan, T.A.M.T., 2002. A fast and elitist multiobjective genetic algorithm: NSGA-II. *IEEE Transactions on Evolutionary Computation*, 6(2): 182-197.
- Eliasson, J., Hultkrantz, L., Nerhagen, L., Smidfelt Rosqvist, L., 2009. The Stockholm congestion-charging trial 2006: Overview of effects. *Transportation Research Part A*, 43(3): 240-250.
- Ferrari, P., 1995. Road pricing and network equilibrium. *Transportation Research Part B*, 29 (5): 357-372.
- Fiske, K., 2011. Accelerating the search for optimal dynamic traffic management. Master's Thesis, University of Twente, The Netherlands.
- Fix NY, 2018. Fix NY Advisory Panel Report. Available at: <http://hntb.com/HNTB/media/HNTBMediaLibrary/Home/Fix-NYC-Panel-Report.pdf>. Accessed: March 28, 2018.
- Forrester, A.I.J. and Keane, A.J., 2009. Recent advances in surrogate-based optimization. *Progress in Aerospace Science*, 45: 50-79.
- Gan, L.P., Recker, W.W. 2008. A mathematical programming formulation of the household activity rescheduling problem. *Transportation Research Part B*, 42(6): 571-606.
- Gutmann, H.M., 2001. A radial basis function method for global optimization. *Journal of Global Optimization*, 19: 201-227.
- Hult, E.E., 2006. Closed charging cordon design problem. University of Cambridge, UK.
- International Transportation Forum, 2010. Reducing transport greenhouse gas emissions: Trends and data 2010. OECD and International Transportation Forum.
- Kitamura, R., C. Chen, R. A. M. M. Pendyala, Narayanan, R., 2000. Micro-simulation of daily activity-travel patterns for travel. *Transportation*, 27: 25-51.
- Lamotte, R.A.F., 2014. A fast multi-objective optimization approach to solve the continuous network design problem with microscopic simulation. Master's Thesis, Concordia University, Canada.
- Levy, J.I., Buonocore J.J., von Stackelberg, K., 2010. Evaluation of the public health impacts of traffic congestion: A health risk assessment. *Environmental Health*, 9(65): 1-12.
- Li, Z.C., Lam, W.H.K., Wong, S.C., Sumalee, A., 2012. Environmentally sustainable toll design for congested road networks with uncertain demand. *International Journal of Sustainable Transportation*, 6: 127-155.

- Li, Z.C., Wang, Y.D., Lam, W.H.K., Sumalee, A., Choi, K., 2014. Design of sustainable cordon toll pricing schemes in a monocentric city. *Networks and Spatial Economics*, 14(2): 133-158.
- Maruyama, T., R. Takaki., Mizokami, S., 2014. Incorporating computational geometry into second-best congestion pricing design problem: Algorithm development and applications. In *Proceedings of the 93rd Transportation Research Board Annual Meeting*, Washington, D.C.
- Miller, E. J., Roorda, M.J., 2003. Prototype model of household activity-travel scheduling. *Transportation Research Record*, 1831: 114-121.
- Nagurney, A., 2000. Congested urban transportation networks and emission paradoxes. *Transportation Research Part D*, 5(2): 145-151.
- Nagurney, A., 2000. *Sustainable transportation networks*. Cheltenham, UK: Edward Elgar
- Osorio, C., Bierlaire, M., 2013. A simulation-based optimization framework for urban transportation problems. *Operations Research* 61(6): 1333–1345.
- Pendyala, R., R. Kitamura, A. Kikuchi, T. Yamamoto, Fujii, S., 2005. Florida activity mobility simulator: overview and preliminary validation results. *Transportation Research Record*, 1921: 123-130.
- Rabl, A., Spadaro, J.V., Holland, M., 2014. *How much is clean air worth? Calculating the benefits of pollution control*. Cambridge, UK: Cambridge University Press.
- Recker, W.W., 1995. The household activity pattern problem: general formulation and solution. *Transportation Research Part B*, 29(1): 61-77.
- Recker, W.W., 2001. A bridge between travel demand modeling and activity-based travel analysis. *Transportation Research Part B*, 35(5): 481-506.
- Recker, W.W., McNally, M.G., Root, G.S., 1986. A model of complex travel behavior: Part I—Theoretical development. *Transportation Research Part A*, 20(4): 307-318.
- Regis, R.G., Shoemaker, C.A., 2007. A stochastic radial basis function method for the global optimization of expensive functions. *INFORMS Journal on Computing*, 19(4):497-509.
- Regue, R., Allahviranloo, M., Recker, W.W., 2015. Understanding household priorities when scheduling activities. Presented at the 94th Annual Meeting of the Transportation Research Board, Washington, D.C. No. 750.
- Rodriguez-Roman, D., Ritchie, S.G., 2017. Accounting for population exposure to vehicle-generated pollutants and environmental equity in the toll design problem. *International Journal of Sustainable Transportation*, <http://dx.doi.org/10.1080/15568318.2016.1266423>.
- SCAG, 2016. Value pricing. <http://transfin.scag.ca.gov/Pages/Value-Pricing.aspx>. Accessed: March 20, 2018.
- Sharma, S., Mishra, S., 2013. Intelligent transportation systems-enabled optimal emission pricing models for reducing carbon footprints in a bimodal network. *Journal of Intelligent Transportation Systems: Technology, Planning, and Operations*, 17(1): 54-64.

- Sumalee, A., 2004. Optimal road user charging cordon design: A heuristic optimization approach. *Computer-Aided Civil and Infrastructure Engineering*, 19: 377-392.
- Tonne, C., Beevers, S.D., Armstrong, B., Kelly, F., Wilkinson, P., 2008. Air pollution and mortality benefits of the London Congestion Charge: Spatial and socioeconomic inequalities. *Occupational and Environmental Medicine*, 65(9): 620-627.
- US EPA, 2014. Inventory of US Greenhouse Gas Emissions and Sinks: 1990-2012. EPA 430-R-14-003, US Environmental Protection Agency, Washington DC.
- US EPA, 2014. Motor Vehicle Emission Simulator (MOVES): user guide for MOVES2014. US Environmental Protection Agency, EPA-420-B-14-055.
- Wang, J.Y.T., Ehrgott, M., Dirks, K.N., Gupta, A., 2014. A bilevel multi-objective road pricing model for economic, environmental and health sustainability. *Transportation Research Procedia*, 3: 393-402.
- Wismans, L.J.J., 2012. Toward sustainable dynamic traffic management. Doctoral Dissertation, University of Twente, The Netherlands.
- World Bank, Institute for Health Metrics and Evaluation, 2014. Transport for health: The global burden of disease from motorized road transport. Institute for Health Metrics and Evaluation and World Bank.
- Xiong, Y., Schneider, J.B., 1992. Transportation network design using a cumulative genetic algorithm and neural network. *Transportation Research Record*, 1364: 37-44.
- Yang, H., Bell, M.G.H., 1997. Traffic restraint, road pricing, and network equilibrium. *Transportation Research Part B*, 31(4): 303-314.
- Yin, Y., Lawphongpanich, S., 2006. Internalizing emission externality on road networks. *Transportation Research Part D*, 11:292-301.
- Yin, Y., Lu, H., 2000. Traffic equilibrium problems with environmental concerns. *Journal of Eastern Asia Society for Transportation Studies*, 3: 195-206.
- Zhang, L., Sun, J., 2013. Dual-based heuristic for optimal cordon pricing design. *Journal of Transportation Engineering*, 139(11): 1105-1116.
- Zhang, X., Yang, H., 2004. The optimal cordon-based network congestion pricing problem. *Transportation Research Part B*, 38: 517-537.
- Bar-Gera, H. Transportation network test problems. <http://www.bgu.ac.il/~bargera/tntp/>. Accessed: January 9, 2014.
- Jayakrishnan, R., Tsai, W.K., Prashker, J.N.M., Rajadhyaksha, S., 1994. A faster path-based algorithm for traffic assignment. *Transportation Research Record*, 1443: 75-83.
- EPA, 2014. Motor Vehicle Emission Simulator (MOVES): User guide for MOVES2014. EPA-420-B-14-055, US Environmental Protection Agency.

Venegas, L.E., Mazzeo, N.A., Dezzutti, M.C., 2014. A simple model for calculating air pollution within street canyons. *Atmospheric Environment*, 87: 77-86.

Khuri, A. I., Mukhopadhyay, S., 2010. Response surface methodology. *Wiley Interdisciplinary Reviews: Computational Statistics* 2(2): 128–149.

A long-exposure photograph of a city skyline at night, viewed from across a body of water. The skyline is filled with illuminated skyscrapers, including a prominent one with a blue facade. In the foreground, a bridge or highway spans the water, with light trails from moving vehicles creating a sense of motion. The overall scene is a blend of urban architecture and transportation infrastructure.

University Transportation Research Center - Region 2
Funded by the U.S. Department of Transportation

**Region 2 - University Transportation
Research Center**
The City College of New York
Marshak Hall, Suite 910
160 Convent Avenue
New York, NY 10031
Tel: (212) 650-8050
Fax: (212) 650-8374
Website: www.utrc2.org